Hi Emma,

Thank you for that.

I have attached two documents as supporting evidence for our PFAS solution.

Kind Regards,

Lauchlan Grout

Co Founder & CEO | Hemp Farms Australia ™

Science of the Total Environment 959 (2025) 178348

Contents lists available at ScienceDirect

Science of the Total Environment

journal homepage: www.elsevier.com/locate/scitotenv

PFAS biodegradation by *Labrys portucalensis* F11: Evidence of chain shortening and identification of metabolites of PFOS, 6:2 FTS, and 5:3 FTCA

Mindula K. Wijayahena [a], Irina S. Moreira [b], Paula M.L. Castro [b], Sarah Dowd [c], Melissa I. Marciesky [d], Carla Ng [d,e], Diana S. Aga [a,f,*,**]

[a] Department of Chemistry, University at Buffalo, The State University of New York, Buffalo, NY 14260, United States
[b] Universidade Católica Portuguesa, CBQF - Centro de Biotecnologia e Química Fina – Laboratório Associado, Escola Superior de Biotecnologia, Rua Diogo Botelho 1327, 4169-005 Porto, Portugal
[c] Waters Corporation, 34 Maple St, Milford, MA 01757, United States
[d] Department of Chemical and Petroleum Engineering, University of Pittsburgh, Pittsburgh, PA 15261, United States
[e] Department of Civil and Environmental Engineering, University of Pittsburgh, Pittsburgh, PA 15261, United States
[f] Research and Education in Energy, Environment and Water (RENEW), University at Buffalo, The State University of New York, Buffalo, NY 14260, United States

HIGHLIGHTS

- Bacterial defluorination and chain shortening of PFOS, 6:2 FTS, 5:3 FTCA occurred
- PFOS removal of up to 96 % was observed after a 194-day incubation period
- After 100 day-incubation, up to 58 % of 5:3 FTCA and 21 % of 6:2 FTS were removed
- Several defluorinated PFOS metabolites were detected during biodegradation

GRAPHICAL ABSTRACT

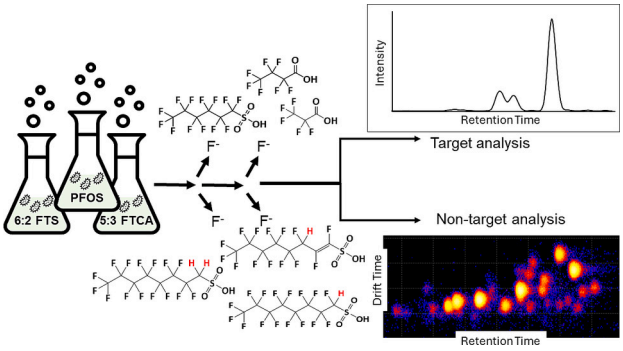

ARTICLE INFO

Editor: Dimitra A Lambropoulou

Keywords:
Per- and polyfluoroalkyl substances
Aerobic biodegradation
Defluorinated metabolites
High-resolution mass spectrometry
Ion mobility separation

ABSTRACT

The biodegradation of three per- and polyfluoroalkyl substances (PFAS), namely perfluorooctane sulfonic acid (PFOS), 6:2-fluorotelomer sulfonic acid (6:2 FTS), and 5:3-fluorotelomer carboxylic acid (5:3 FTCA), were evaluated using *Labrys portucalensis* F11, an aerobic bacteria known to defluorinate fluorine-containing compounds. Cultures of *L. portucalensis* F11 were grown in minimal salts media and treated with 10,000 μg/L of individual PFAS as the sole carbon source in separate flasks. In PFOS-spiked media, several metabolites were detected, including perfluoroheptane sulfonic acid (PFHpS), perfluorohexane sulfonic acid (PFHxS), perfluorohexanoic acid (PFHxA), perfluoropentanoic acid (PFPeA), perfluorobutanoic acid (PFBA), and perfluoropropanoic acid (PFPrA). After 194-day incubation three de-fluorinated metabolites were identified: PFOS-F (m/z = 480.940, PFOS-2F (m/z = 462.980), and unsaturated PFOS-3F (m/z = 442.943). During the

* Corresponding author at: Department of Chemistry, University at Buffalo, The State University of New York, Buffalo, NY 14260, United States.
** Corresponding author at: Research and Education in Energy, Environment and Water (RENEW), University at Buffalo, The State University of New York, Buffalo, NY 14260, United States.
E-mail address: dianaaga@buffalo.edu (D.S. Aga).

https://doi.org/10.1016/j.scitotenv.2024.178348
Received 3 October 2024; Received in revised form 24 December 2024; Accepted 29 December 2024
Available online 4 January 2025
0048-9697/© 2025 Elsevier B.V. All rights are reserved, including those for text and data mining, AI training, and similar technologies.

biodegradation of 5:3 FTCA, the following metabolites were observed: PFHxA, PFPeA, PFBA, PFPrA, and two fluorotelomer unsaturated carboxylic acids (5:3 FTUCA and 7:2 FTUCA). The biodegradation of 6:2 FTS was slower, with only 21 % decrease in concentration observed after 100 days, and subsequent formation of 4:2 FTS. On the contrary, 90 % of PFOS and 58 % of 5:3 FTCA were degraded after 100 days. These results indicate that *L. portucalensis* F11 can be potentially used for PFAS biodegradation in contaminated environments.

1. Introduction

Per- and polyfluoroalkyl substances (PFAS) are a class of highly fluorinated synthetic organic chemicals that have been extensively used in industrial, commercial, and domestic applications for over several decades now due to their surfactant-like, water-repellant, and oleophobic properties (Buck et al., 2011). The carbon-fluorine bonds characteristic of PFAS exhibit very high bond dissociation energies: around 485 kJ/mol, making PFAS generally resistant to degradation by oxidation, thermal treatment, and biological mechanisms; hence PFAS has been dubbed as "forever chemicals" (Brunn et al., 2023). PFAS can bioaccumulate in humans and animals following repetitive exposure (Taniyasu et al., 2003), leading to adverse health outcomes. These effects include thyroid disorders, immunotoxicity, neurotoxicity, and association with various types of cancer (Grandjean, 2018; Grandjean et al., 2020; Lewis et al., 2015; Vieira et al., 2013; Rios-Bonilla et al., 2024). The stability, vast applications, and improper waste disposal have made PFAS ubiquitous environmental pollutants (Barzen-Hanson et al., 2017; Prevedouros et al., 2006; Taniyasu et al., 2003) and requires costly remediation efforts (Cordner et al., 2021).

Strategies to enhance the biodegradation of PFAS are of great interest, particularly through bioaugmentation using microorganisms to degrade pollutants (Muter, 2023; Nzila et al., 2016). Bioaugmentation has been successfully implemented in soil bioremediation (Bokade et al., 2023; Dagliya et al., 2022), wastewater treatment (Chen et al., 2022; Dutta et al., 2022), and air biofiltration (Muter, 2023). However, there is limited information on the microbial degradation of fluorinated compounds, especially PFAS. Identifying microorganisms capable of degrading PFAS, evaluating their efficiency, and characterizing biodegradation products are critically needed because of the lack of cost-effective remediation technologies capable of removing PFAS in contaminated environments.

Recent studies have shown that microbial communities can defluorinate certain PFAS, suggesting that natural microbial defluorination exists (Yu et al., 2020). For instance, *Acidimicrobium* sp. strain A6 (A6) was found to reduce perfluorooctane sulfonic acid (PFOS) and perfluorooctanoic acid (PFOA) in enriched cultures under anaerobic conditions (Huang and Jaffe, 2019). However, isolating the specific microorganisms responsible for PFAS biodegradation from mixed cultures can be challenging, especially if they are present at low abundance, making them difficult to identify and enrich. A recent study reported defluorination of α, β-unsaturated PFAS by *Acetobacterium* spp. (Yu et al., 2024), but only measured the increase in fluoride ion concentrations in the media without characterizing the metabolites formed during biodegradation of PFAS. Various *Pseudomonas* spp. have been shown to degrade some PFAS under aerobic conditions. For instance, *Pseudomonas parafulva* YAB1 resulted in 48 % reduction in PFOA over a 96-day incubation, but no biodegradation products nor fluoride ions were measured (Yi et al., 2016). Another study showed that *Pseudomonas aeruginosa* strain HJ4 isolated from the sludge of a municipal wastewater treatment plant decreased the concentration of PFOS by up to 67 % in 48 h (Kwon et al., 2014). However, no fluoride production was observed, and no major biodegradation products were uncovered, leaving one to suspect that the decrease in PFOS could be mostly due to adsorption rather than biodegradation. Another study demonstrated *Pseudomonas plecoglossicida* 2.4-D degraded PFOS by 75 %, increasing fluoride ions in the growth media, but also did not specify the degradation products formed (Chetverikov et al., 2017). Additional information on bacterial degradation of PFAS under aerobic conditions from literature are listed in Table 1. Taking into account the aforementioned evidence, there is a need to identify microbial strains that have the ability to degrade PFAS and to characterize degradation products formed to assess their potential for PFAS bioremediation in highly contaminated sites.

This study investigates the ability of *Labrys portucalensis* F11, an aerobic bacterial strain from the Xanthobacteraceae family, to biodegrade three types of PFAS (listed in Fig. 1). Isolated from Estarreja, Portugal, *L. portucalensis* F11 has demonstrated metabolic versatility, effectively degrading fluorobenzene (Carvalho et al., 2008), 1,2-, 1,3-, and 1,4-difluorobenzenes (Moreira et al., 2012a), and fluorinated pharmaceuticals such as ofloxacin, norfloxacin, and ciprofloxacin (Amorim et al., 2014). Additionally, this bacterial strain can degrade fluoxetine, releasing fluoride from the perfluorinated methyl group ($-CF_3$) (Moreira et al., 2014). Therefore, the current study investigated the ability of *L. portucalensis* F11 to biodegrade 8-carbon chain PFAS with different headgroups and degree of fluorination on the carbon chain: 6:2-fluorotelomer sulfonic acid (6:2 FTS), 5:3-fluorotelomer carboxylic acid (5:3 FTCA), and PFOS, with structures shown in Fig. 1.

PFOS was chosen as the main test compound due to its high environmental abundance, frequent detection in biological samples, bioaccumulative nature, and known toxicity (Buck et al., 2011; Brunn et al., 2023). The study also included 6:2 FTS and 5:3 FTCA to compare the biodegradability of polyfluorinated versus perfluorinated substances, and the impact of different head groups (sulfonate vs. carboxylate). Further, there have been reports indicating that the presence of carbon without fluorine in PFAS makes them more biodegradable (Harding-Marjanovic et al., 2015; Zhang et al., 2016). Biodegradation was evaluated by measuring the decrease in PFAS concentrations and identifying biotransformation products using liquid chromatography with tandem mass spectrometry (LC-MS/MS) and ion mobility separation coupled with high-resolution mass spectrometry (IMS-HRMS). The results indicate that *L. portucalensis* F11 can defluorinate and shorten the chains of both poly- and perfluorinated PFAS, including those with sulfonated and carboxylated headgroups, highlighting the potential of this bacterial strain for bioremediation applications in PFAS-contaminated sites.

2. Materials and methods

2.1. Chemicals and reagents

Minimal salts medium (MM) was prepared with analytical grade chemicals (Sigma–Aldrich Saint Louis, MO) according to (Moreira et al., 2012b) without modification. PFOS and 6:2 FTS, were purchased from Sigma Aldrich (Saint Louis, MO) while 5:3 FTCA was purchased from SynQuest laboratories, Inc. (Alachua, FL). Other details can be found in Supporting Information (SI).

2.2. Microorganism

The bacterial strain *L. portucalensis* F11 (GenBank/EMBL/DDBJ accession number AY362040; DSMZ accession number DSM 17916) was isolated from a sediment sample collected from an industrially contaminated site in Northern Portugal (Carvalho et al., 2008). This microorganism was selected for the biodegradation of PFAS due to its demonstrated ability to degrade fluorinated pharmaceuticals and fluorobenzenes (Amorim et al., 2014; Carvalho et al., 2008; Moreira et al.,

2012a; Moreira et al., 2014). The microorganism was routinely cultivated on nutrient agar (NA) plates incubated for 2 days at 30 °C to prepare the inoculum for the biodegradation experiments.

2.3. Biodegradation experiments

Biodegradation of PFOS, 6:2 FTS, and 5:3 FTCA by strain *L. portucalensis* F11 was carried out under aerobic conditions in 250 mL sealed flasks containing 50 mL of MM supplemented with 10,000 μg/L of PFOS, 6:2 FTS, and 5:3 FTCA, separately. Cells of *L. portucalensis* F11 were inoculated at an optical density (OD) of about 0.05 at 600 nm, and bacterial growth was monitored by measuring OD spectrophotometrically (Helios Gamma, Unicam Instruments, UK).

All the cultures were incubated at 30 °C on a rotary shaker (130 rpm). Experiments were performed in duplicate under sterile conditions. Abiotic control assays consisted of sealed flasks containing MM supplemented with 10,000 μg/L of PFOS, 6:2 FTS, and 5:3 FTCA separately, without bacterial inoculation. A control for cell growth was established with three flasks with the same concentration of methanol without PFOS, 6:2 FTS, and 5:3 FTCA addition. Samples were sacrificed for analysis at 0, 48, 100, and 194 days to assess microbial growth and PFOS, 6:2 FTS, and 5:3 FTCA biodegradation. The purity of the cultures was evaluated through regular plating on NA plates. Abiotic control experiments were conducted for PFOS and 5:3 FTCA incubating for 48-days. These experiments were performed under the same conditions as described above but without the presence of bacteria.

2.4. Analytical methods

2.4.1. Fluoride analysis

For each flask sacrificed for analysis, biomass was removed from culture samples by centrifugation at 14,000 rpm for 10 min at 4 °C. The concentration of fluoride ions in the supernatant was monitored weekly using an ion-selective electrode (model Orion 96-09, Thermo Electron Corporation, Beverly, MA), as previously described by (Moreira et al., 2014).

2.4.2. Solid phase extraction

Each of the culture supernatant (30 mL) was extracted and preconcentrated through solid phase extraction (SPE) using Oasis® HLB and Resprep® MCX cartridges in tandem (HLB-WAX SPE), as described in our earlier works (Guardian et al., 2020; Halwatura and Aga, 2023). Detailed process can be found in the SI. Extraction recovery percentages, the method limits of detection (LOD) and limits of quantification (LOQ) can be found in our previous works (Guardian et al., 2020; Halwatura and Aga, 2023).

2.4.3. Target analysis by liquid chromatography - tandem mass spectrometry (LC-MS/MS)

Target analysis for 40 PFAS (listed in Table S1) was carried out using the LC-MS/MS method described in our previous publication (Camdzic et al., 2023), and concentrations were determined using isotope dilution with ^{13}C-labeled PFAS analogues (MPFAC – 24 ES). Detailed instrument parameters can be found in the SI. To prevent potential contamination, materials containing polytetrafluoroethylene (PTFE) were excluded. Each run incorporated blank injections following each PFAS sample injection, along with extraction blanks and quality control check standards, including a 50 μg/L PFAS standard mix. Throughout the runs, the areas of the analyte peaks, chromatographic retention times, and background contaminations were closely monitored.

2.4.4. Non-target analysis using ultra performance liquid chromatography with ion mobility separation coupled to a time-of-flight mass spectrometer (UPLC/IMS-QToF/MS)

To determine the formation of PFAS metabolites that were not included in the targeted PFAS analysis, a non-target analysis approach was performed using a Waters™ Acquity Ultra Performance Liquid Chromatograph with a SELECT SERIES™ cyclic ion mobility-quadrupole-time-of-flight mass spectrometer (UPLC/IMS-QToF/MS) adopting a procedure described by (Organtini et al., 2023). A 5.0-μL sample was injected into the Atlantis™ Premier BEH™ C18 AX analytical column (100 × 2.1 mm × 1.7 μm) obtained from Waters Technology Corporation (Milford, MA). Gradient chromatography was performed using a flow rate of 0.30 mL/min with 2 mM ammonium acetate in Nanopure™ water (mobile phase A) and 0.1 % ammonium hydroxide in methanol (mobile phase B). Details of the UPLC/IMS-QToF/MS mobile phase conditions and MS parameters are described in SI, Table S2, and Table S3.

3. Results and discussion

High starting concentrations of PFAS that exceed typical levels found in environments were utilized for several critical reasons. Firstly, higher concentrations enable us to observe changes in the substance's concentration and detection of metabolites formed without preconcentration. Secondly, elevated concentrations help the microbial community adapt to the substance, reducing the initial lag phase during which minimal degradation occurs (Özel Duygan et al., 2021). While the spiking PFAS concentration used in this study is not typical in the natural environment, PFAS concentrations can reach up to hundreds of mg/

Table 1
Microbial transformation of perfluoroalkyl sulfonic acids and polyfluoroalkyl sulfonic acids under aerobic conditions from literature.

PFAS	Microbial strain	Incubation time (days)	% of removal of starting PFAS	Transformation products	Reference
Perfluoroalkyl sulfonic acids					
PFHxS	*Pseudomonas strains* PS27 and PDMF10	7	~30–40 % reduction of bioaccumulation	–	(Presentato et al., 2020)
PFOS	*Pseudomonas aeruginosa* HJ4	48	67	PFHxS, PFBS	(Kwon et al., 2014)
	Pseudomonas plecoglossicida 2.4-D	6	In liquid media- ~100	PFHpA, F^-	(Chetverikov et al., 2017)
	Pseudomonas plecoglossicida 2.4-D	~180	In soil- 75	–	
Polyfluoroalkyl sulfonic acids					
6:2 FTS	*Gordonia* sp. NB4-1Y	7	99.9	6:2 FTCA ($C_6F_{13}CH_2CO_2H$), 6:2 FTUCA ($C_4F_{11}CF{=}CHCO_2H$), 5:3 FTCA, 4:3 FTCA, PFHxA, PFPeA, PFBA	(Shaw et al., 2019)
	Rhodococcus jostii RHA1	~3	99	6:2 FTUCA, α-OH 5:3 FTCA, PFHpA, 6:2 FTUSA, ($C_6F_{13}CH{=}CHSO_3H$)	(Yang et al., 2022)
	Enrich with *Dietzia aurantiaca* J3	7	~100	6:2 FTCA, 6:2 FTUCA, 5:3 FTCA, PFHxA, PFPeA, F^-	(Mendez et al., 2022)

L levels in manufacturing wastes (Prevedouros et al., 2006) and in spent granulated activated carbon (DiStefano et al., 2022).

3.1. Evidence of defluorination and chain-shortening of PFAS

A significant increase in the concentration of F^- (114 μg/L: 2 % of defluorination) was observed for PFOS after 48 days of incubation, which increased further in the last sample collected at 194 days (219 μg/L: 3 % of defluorination). Removal of up to 96 % of the initial PFOS was also observed after 194-day incubation, indicating biodegradation of PFOS by *L. portucalensis* F11. The increase in fluoride ion concentration and a corresponding decrease in PFOS over the period of incubation is shown in Fig. 2A.

Defluorination of 6:2 FTS and 5:3 FTCA by *L. portucalensis* F11 were also observed. Analysis of the culture media spiked with 6:2 FTS collected after 100-day incubation revealed increase in F^- concentration (76 μg/L: 1 % of defluorination) and a corresponding decrease in 6:2 FTS concentration (Table S6); the 48-day sample did not have detectable F^- and was therefore not analyzed by LC-MS/MS. Similarly, decrease in 5:3 FTCA over the period of 100 days was accompanied by increase in fluoride ions, with concentration reaching 86 μg/L (1 % of defluorination) (Fig. 2C) at the end of the incubation period. Both concentrations of 6:2 FTS and 5:3 FTCA decreased in the culture media by 21 % and 58 % respectively, at around 100 days of incubation (Fig. 6).

The cell growth pattern was very similar in all the tested conditions, in the presence or absence (growth control) of PFAS, with the maximum OD_{600} of 0.233 ± 0.017 observed at 48 days. There was no evidence that the degradation of PFAS contributed to the growth of the bacteria; however, at the concentrations of PFOS, 6:2 FTS, and 5:3 FTCA used in the experiments, the amount of carbon could be too low to support bacterial growth. On the other hand, there was also no evidence of the toxic effect of the tested PFAS on *L. portucalensis* F11 cells, as the presence of these compounds did not affect growth.

No fluoride release was observed in the abiotic control, indicating that chemical or photolytic degradation of PFAS did not occur in the absence of *L. portucalensis* F11 cells. The abiotic controls for PFOS and 5:3 FTCA showed only around 0.2 % decrease in the corresponding PFAS in the culture media, indicating that the loss of spiked PFAS during the experimental procedure is negligible and there is no significant adsorption to the glassware. Data obtained from the biomass (Table S4) also showed that no significant amount of PFAS accumulated in the bacterial cells.

3.2. Biodegradation of PFOS and formation of metabolites

The spiked PFOS used as sole carbon source by *L. portucalensis* F11 was biodegraded into shorter chain metabolites, which were detected across the sampling points at 48, 100 and 194 days. Target analysis of the 48-day culture media revealed the formation of perfluoroheptane sulfonic acid (PFHpS), perfluorohexane sulfonic acid (PFHxS), perfluorohexanoic acid (PFHxA), perfluoropentanoic acid (PFPeA), perfluorobutanoic acid (PFBA), and perfluoropropanoic acid (PFPrA) (Fig. 2B). The metabolites detected in the target analysis matched the retention times of the isotopically labeled standards, as well as the expected MS/MS fragmentation pattern and ion ratios of the PFAS standards. Similar transformation products were detected for the repeated 6:2 FTS and 5:3 FTCA spiked samples for 194-day incubation (Table S5).

The production of perfluorocarboxylic acids (PFCAs) indicates that during the biodegradation of PFOS, the sulfonic acid head group is converted to a carboxylic acid group, as indicated in the proposed biotransformation pathway in Fig. 3. Based on a previous study (Cook et al., 1998), desulfonative enzymes in aerobic bacteria are generally regulated by induction when the sulfonate acts as a carbon and energy source, or by a global sulfur scavenging network when the sulfonate is utilized as a sulfur source. Further, the formation of carboxylated metabolites may have been promoted by the enzymatic activities of the bacteria as discussed by Yang et al. (2022). Another study suggested that the increased concentration of acetate in the culture media accompanies the biodegradation of PFOS (Huang and Jaffe, 2019), which may have promoted the formation of carboxylated metabolites. In proposing degradation pathways based on the metabolites identified in this study, we conducted a comparison with other PFAS-degrading bacteria and analyzed various degradation pathways to strengthen our findings. Table 1 summarizes the microbial transformation of perfluoroalkyl sulfonic acids, polyfluoroalkyl carboxylic acids, and polyfluoroalkyl sulfonic acids under aerobic conditions, as reported in the literature. These literature findings are consistent with our results and proposed degradation pathways.

The detection of shorter-chain PFAS in the culture media, along with the increased formation of fluoride ions, clearly indicate that *L. portucalensis* F11 has the ability to degrade PFOS. However, we hypothesize that the concentrations of the detected shorter-chain PFAS shown in Fig. 2B are underestimated because there may be other metabolites that have escaped detection by LC-MS/MS, including those that are volatile. The volatility of carboxylated PFAS increases with a decrease in chain length, resulting in loss to the atmosphere at the culture temperatures used (Mancinelli et al., 2023). In fact, the data from the second set of experiments (Table S5) showed the formation of shorter-chain PFAS, trifluoroacetic acid (TFA) and PFPrA, supporting our hypothesis. Unlike the first set, the samples from this second set of experiments were shipped and analyzed immediately, and were not stored for a prolonged period of time.

3.3. Identification of additional by-products of PFOS by non-target analysis

Non-target analysis using HRMS combined with IMS was used to identify other metabolites that were not included in the targeted analysis. Adding IMS gives the possibility to resolve species of interest from coeluting matrix interferences and separate structural isomers based on their collision cross section (CCS) (Izquierdo-Sandoval et al., 2022). Measured drift times (DT) in the IMS cell can be used to calculate CCS values that can serve as an additional parameter for identifying unknown metabolites. Based on the detected amounts of targeted PFAS metabolites, the remaining PFOS concentration, and the released F^- in the culture media, much of the fluorine content of the spiked PFAS remained unaccounted for.

While many peaks were detected with non-targeted analysis, a few major peaks of interest were selected for identification. Previous studies have demonstrated that compounds containing halogens such as fluorine occupy a unique space in the plots of CCS vs *m/z* values because halogenated compounds have smaller CCS values than compounds without halogen with the same *m/z* (Dodds et al., 2020; Foster et al., 2022; MacNeil et al., 2022; Mullin et al., 2020).

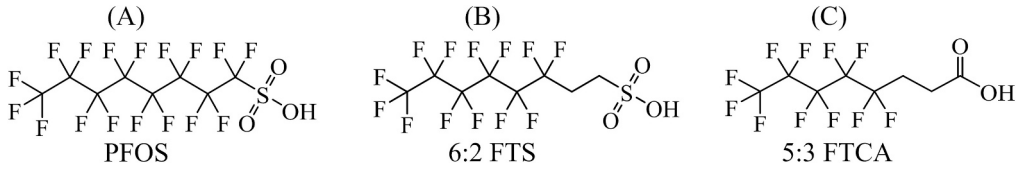

Fig. 1. Structures of A) perfluorooctane sulfonic acid (PFOS), B) 6:2-fluorotelomer sulfonic acid (6:2 FTS), and C) 5:3-fluorotelomer carboxylic acid (5:3 FTCA).

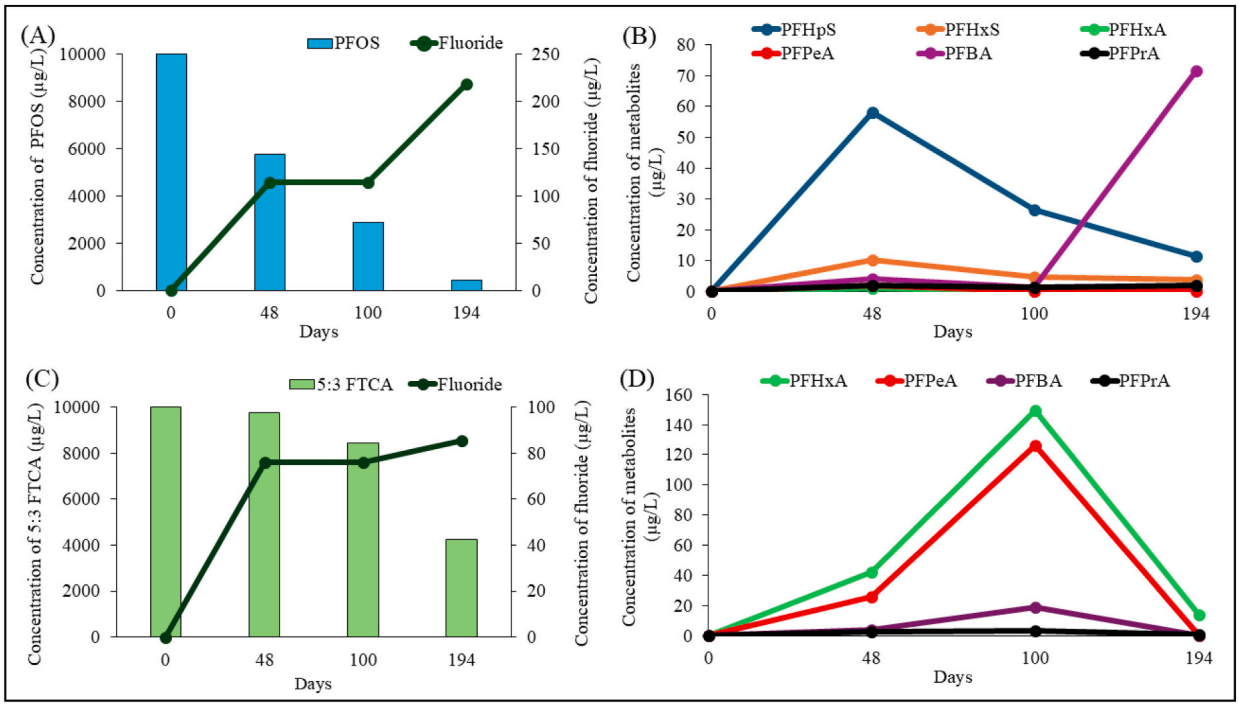

Fig. 2. Plot showing the decrease in PFOS and the corresponding increase in fluoride ions (A), the formation of shorter-chain PFAS metabolites (PFHpS, PFHxS, PFHxA, PFPeA, PFBA and PFPrA) from PFOS biodegradation (B) plot showing the decrease in 5:3 FTCA and the corresponding increase in fluoride ions (C), the formation of shorter-chain PFAS metabolites (PFHxA, PFPeA, PFBA and PFPrA) from 5:3 FTCA biodegradation (D) detected at 0, 48, 100, and 194 days of incubation.

As a starting point, the PFOS sample from the 194-day incubation was screened because it exhibited the highest number of metabolites detected by targeted LC-MS/MS analysis. Interestingly, non-targeted analysis identified three new additional metabolites of PFOS (Fig. 3). Each detected metabolite was assigned a corresponding confidence level based on the experimental *m/z* ratio, fragmentation pattern, retention time, mass defect, and isotopic pattern, as described in a previous publication (Charbonnet et al., 2022). The first metabolite identified (PFOS-F) had the formula of $C_8H_2F_{16}O_3S$, indicating the substitution of one fluorine with a hydrogen atom. The observed *m/z* value for the [M-H]- adduct for PFOS-F (*m/z* = 480.940) matched the theoretical *m/z* within 5 ppm error. Fragment ions detected in the high collision energy spectrum of this compound matched the theoretical fragmentation of the proposed structure (Fig. S1). The PFOS-F detection was therefore assigned a confidence level of 3a because the location of the hydrogen substitution remains ambiguous.

The second metabolite (PFOS-2F) was tentatively identified with the formula of $C_8H_3F_{15}O_3S$ where two fluorine atoms in PFOS were substituted with two hydrogen atoms. The observed *m/z* for PFOS-2F (*m/z* = 462.980) matched the theoretical *m/z* value within 5 ppm error, and the MS/MS fragmentation matched the proposed structure (Fig. S2). Consequently, the PFOS-2F detection was assigned a confidence level of 3a because the locations of the hydrogen substitutions also remain ambiguous.

Lastly, a third metabolite (PFAS-3F) was tentatively identified with the formula of $C_8H_2F_{14}O_3S$; an unsaturated PFOS resulting from defluorination and dehydrogenation with a measured mass (*m/z* = 442.943) that matched the theoretical *m/z* value within 5 ppm error (Fig. S3). While more than 3 diagnostic fragment ions were detected, the confidence level was also assigned as 3a because the locations of defluorination and unsaturation in the molecule remain ambiguous.

Many PFAS, including PFOS, exist as branched and linear isomeric mixtures in natural environments due to their manufacturing process (Benskin et al., 2010; Dodds et al., 2020). The PFOS standard used as the carbon source for *L. portucalensis* F11 was a mixture of these linear and branched isomers which are partially separated chromatographically (Fig. 4A). Ion mobility spectrometry provides an extra dimension of separation and allows the separation of the branched PFOS isomers. Coupling LC separation with 6 passes in the cyclic IMS device (IMS resolution ~159 Ω/ΔΩ) revealed over 11 isomers of PFOS (Fig. 4A).

The defluorination processes and the subsequent formation of double bonds can occur in any of the isomers of PFOS, which results in metabolites that consist of numerous structural isomers with different CCS values; these isomers may be separated based on their CCS values using UPLC/IMS-QToF/MS. The use of IMS with 3 passes in the cyclic device (IMS resolution ~112 Ω/ΔΩ) to characterize the defluorinated metabolites of PFOS revealed the presence of at least 9 isomers, for PFOS-F (Fig. 4B), with possibly more at lower intensities. For PFOS-3F analysis using 3 passes in the cyclic device (IMS resolution ~112 Ω/ΔΩ), at least 13 isomers were observed (Fig. 4C). The formation of isomers during metabolism likely results from the bacterial strain's ability to remove fluoride from any carbon, and the potential to form the double bond at any place along the carbon backbone of PFOS. Results from these analyses suggest that while chain shortening is an important degradation pathway, transformation into defluorinated by-products of the same chain length might be as equally important during the biodegradation of PFOS. It is notable that only 3 % of fluoride ions were detected in the media, even after a 90 % decrease in PFOS was observed. While the identified degradation products suggest chain-shortening and dehalogenation as important biodegradation pathways it was difficult to quantify how much of the parent PFAS were actually converted to dehalogenated PFAS because quantification of metabolites was not possible without standards. Similarly, mass balance based on quantification of fluoride ions released was not achieved using the current set-up, hence it is not possible to accurately determine what the main degradation pathway is and is outside the scope of this study.

3.4. Degradation of sulfonated (6:2 FTS) and carboxylated (5:3 FTCA) fluorotelomers

Additional studies were performed to assess the ability of *L. portucalensis* F11 to degrade other PFAS and to determine the

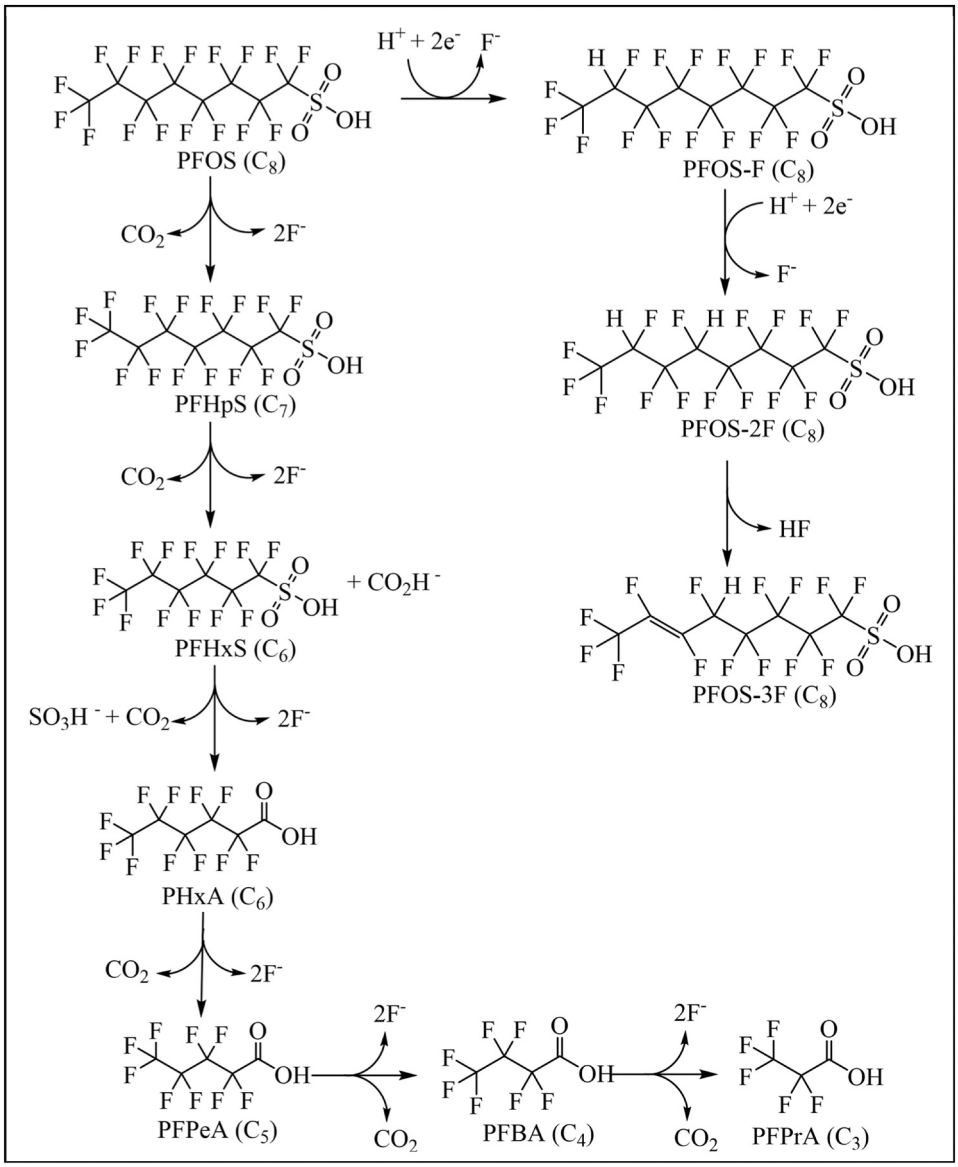

Fig. 3. Proposed biotransformation pathway for PFOS, showing the formation of detected metabolites, during the biodegradation by *L. portucalensis* F11. Defluorination, desulfonation, carboxylation, dehydrogenation, and chain-shortening of PFOS were observed. The number of carbons in the backbone chain is indicated inside the parenthesis to indicate the shortening of PFAS during biodegradation. PFOS-F, PFOS-2F, and PFOS-3F were identified at confidence level 3a, while the others were identified as level 1.

influence of headgroup and degree of fluorination. Hence, separate bacterial cultures were treated with 6:2 FTS and 5:3 FTCA, both of which are 8-carbon chain fluorotelomers, but with different headgroups. When fluoride ions were detectable in cultures, samples were harvested and analyzed by target LC-MS/MS. Hence, the initial sample (0-day incubation) and final sample (~100-day incubation) cultures treated with 6:2 FTS and 5:3 FTCA were analyzed by LC-MS/MS.

Removal of up to 21 % of the initial 6:2 FTS was observed in the final sample Fig. 6; 6:2 FTS concentrations in the spiked cultures decreased with time while the detected free fluoride in the culture media was observed above the limit of detection (Table S6). Over 100 days, the shorter chain fluorotelomer 4:2 FTS (Table S6) was detected as a metabolite as shown in Fig. 5, demonstrating that the spiked 6:2 FTS was degraded by the *L. portucalensis* F11. The metabolite matched the retention time, MS/MS fragmentation pattern, and ion ratio of the corresponding PFAS standard 4:2 FTS. The formation of short-chain metabolite by defluorination and decarboxylation is shown in Fig. 5.

Removal of up to 58 % of the initial 5:3 FTCA was observed in the final sample Fig. 6; 5:3 FTCA concentrations in the spiked cultures decreased with time (Fig. 2C) while the detected free fluoride in the culture media increased. The 5:3 FTCA biodegradation products were shorter chain PFAS, including PFHxA, PFPeA, PFBA, and PFPrA, and were detected over 100 to 194-day incubation (Fig. 2D), demonstrating that the spiked 5:3 FTCA was degraded by the *L. portucalensis* F11 (Fig. 7). Similar transformation products with closer concentrations were detected for the repeated 6:2 FTS and 5:3 FTCA spiked samples for 194-day incubation (Table S5).

The metabolites detected in the targeted analysis matched the retention times of the isotopically labeled standards, MS/MS fragmentation pattern, and ion ratios with corresponding PFAS standards. The MS/MS fragmentation pattern and retention times of the metabolites also matched the corresponding standards. However, as noted above it is likely that the concentrations of the detected shorter-chain PFAS are underestimated because there may be other metabolites that could have escaped detection by target LC-MS/MS, including those that are volatile.

The 5:3 FTCA final sample was used for non-target analysis as it

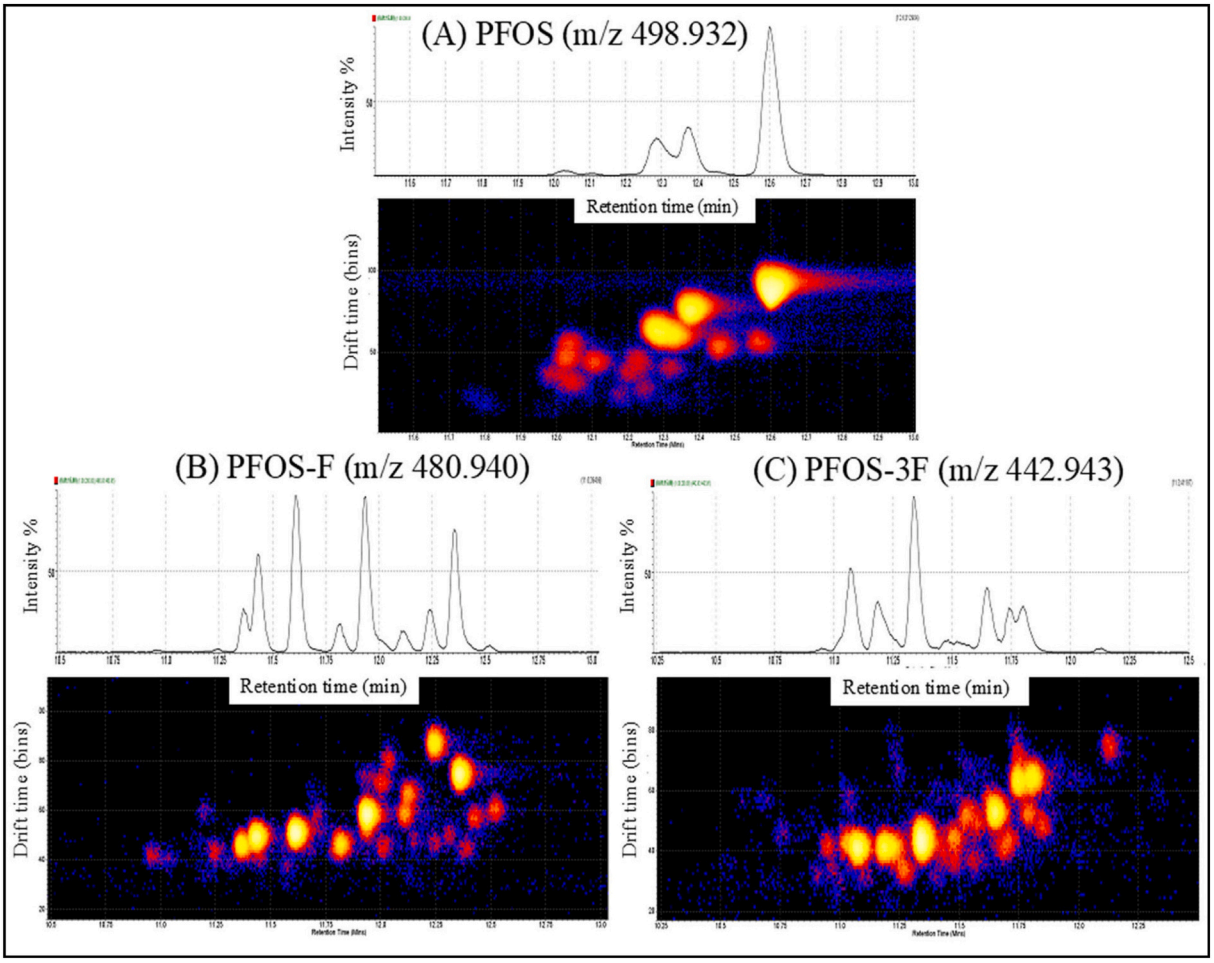

Fig. 4. Extracted ion chromatograms (top figure) and extracted ion mobilograms (bottom figures) exhibiting separation of (A) isomers of PFOS (m/z = 498.932), and isomers of defluorinated PFOS: (B) Isomers of PFOS-F (m/z = 480.940), and (C) Isomers of PFOS-3F (m/z = 442.942). Mobilograms are plots of drift times versus retention times for the selected m/z.

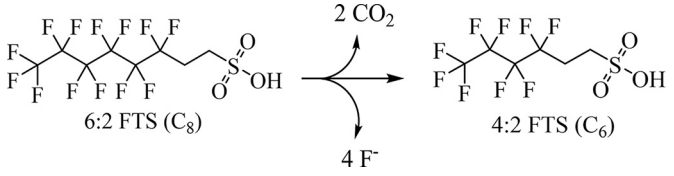

Fig. 5. Proposed biotransformation pathways of detected metabolites detected during the biodegradation of 6:2 FTS by *L. portucalensis* F11 using targeted analysis by Liquid chromatography - Tandem mass spectrometry (LC-MS/MS). All the compounds were identified as confidence level 1.

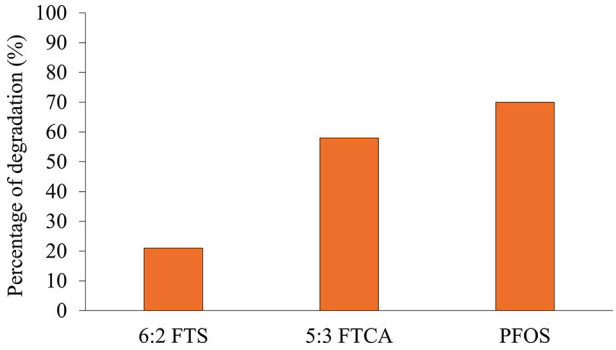

Fig. 6. Plot showing the percentage of degradation of 6:2 FTS, 5:3 FTCA, and PFOS in the final sample (100-day incubation) by *L. portucalensis* F11 bacterial strain.

exhibited the highest number of metabolites detected during targeted LC-MS/MS analysis. Interestingly, the non-targeted analysis identified two metabolites of 5:3 FTCA in addition to those detected via targeted analysis (Fig. 7). The first putative metabolite was assigned with the formula $C_8H_3F_{11}O_2$ and a proposed structure of 5:3 fluorotelomer unsaturated carboxylic acid (5:3 FTUCA), resulting from dehydrogenation. The observed m/z value for the 5:3 FTUCA (m/z = 338.990) matched the theoretical m/z within 5 ppm, and the high collision energy fragmentation had diagnostic ions at 10.83-min (Fig. S4). The 5:3 FTUCA detection was therefore assigned a confidence level of 2b.

The second metabolite of 5:3 FTCA was one carbon shorter and assigned with a formula $C_7H_2F_{10}O_2$ (m/z = 306.982), this was tentatively identified as 5:2 fluorotelomer unsaturated carboxylic acid (5:2 FTUCA). The identification of this metabolite was assigned a confidence level of 2b. The observed fragmentation pattern of 5:2 FTUCA in the high collision energy spectrum (Fig. S5) matched that of a reference standard for 6:2 FTUCA. Additionally, the observed CCS of the tentatively identified 5:2 FTUCA sits on the trendline created when plotting CCS vs m/z with the measured CCS values of 6:2 FTUCA and 8:2 FTUCA (Fig. S6). Subclasses of PFAS with the same headgroup have distinct mass/CCS trendlines (Dodds et al., 2020), and seeing that the value for the proposed identification of 5:2 FTUCA is on this trendline gives increased confidence in its identification. During the non-target analysis

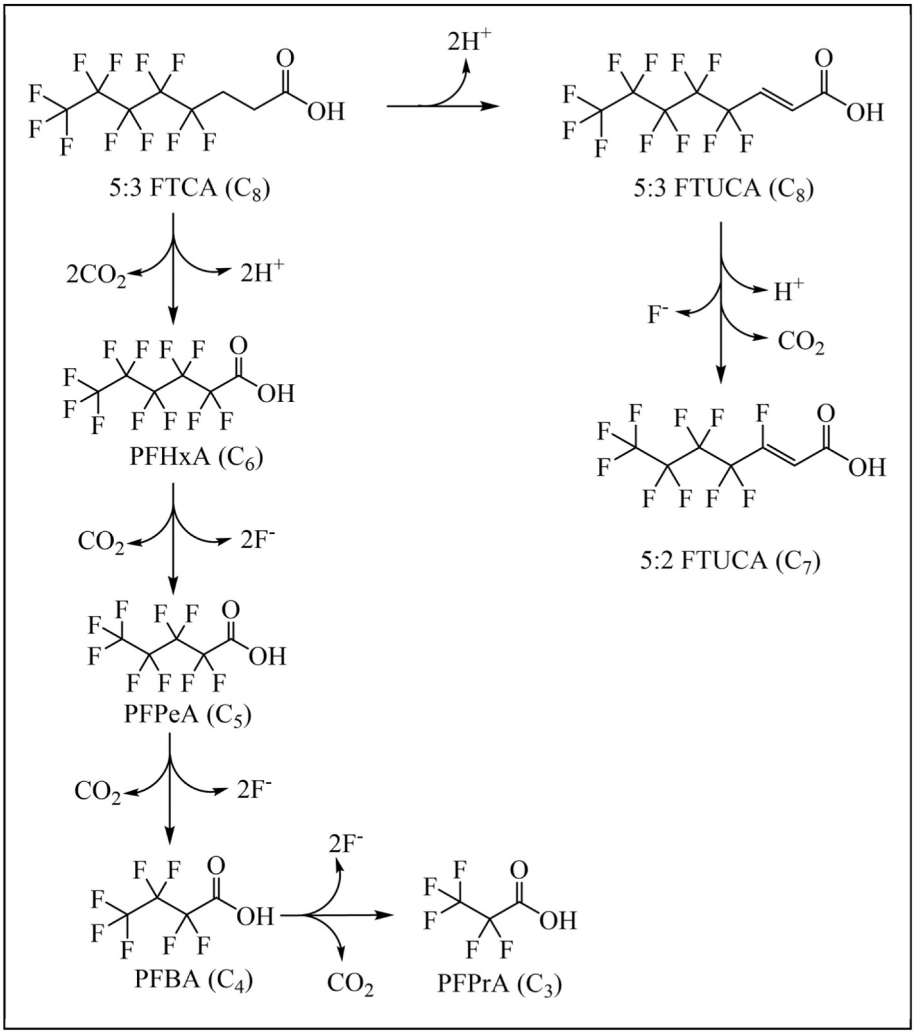

Fig. 7. Proposed biotransformation pathways of detected metabolites formed during the biodegradation of 5:3 FTCA by *L. portucalensis* F11 showing defluorination, hydrogenation, and decarboxylation. The 5:3 FTUCA and 5:2 FTUCA were identified with confidence level 2b while the others were identified with level 1.

of the 194-day incubation 5:3 FTCA sample, isomeric products as we demonstrated for PFOS (Fig. 4) were not identified.

In this study, the combined results from target and non-target analysis demonstrated the remarkable ability of *L. portucalensis* F11 to cleave the strong and stable C—F bonds present in PFOS, 6:2 FTS and 5:3 FTCA as shown in Fig. 3, Fig. 5, and Fig. 7 respectively. PFOS possesses a sulfonic acid head group, while 5:3 FTCA contains a carboxylic acid head group; despite the differences in head group chemistry, we observed the formation of biodegradation products, including shorter-chain PFAS, for the three tested compounds.

3.5. Environmental implications

The results of this study demonstrated that this bacterial strain may be a good candidate for bioremediation of PFAS-contaminated sites, such as in bioaugmentation strategies. *L. portucalensis* F11 may also be potentially used for seeding activated sludge in wastewater treatment plants, especially in the treatment of industrial wastes from manufacturing companies or in the semiconductor industries where PFAS are used in large quantities and end up in wastewater (Ober et al., 2022). As this aerobic bacterial strain was isolated from industrial waste-contaminated sites (Carvalho et al., 2008), it is well adapted to harsh environmental conditions extending its applicability in highly contaminated sites. The strain is able to grow at a temperature range of 16–37 °C and a pH range of 4.0–8.0 (Carvalho et al., 2008), which confers a great potential for adaptation to various environmental conditions.

In this study, we showed the formation of several structural isomers resulting from the biodegradation of PFOS. These findings have several important implications because the federal regulations on the occurrence of PFAS in the environment are implemented only for the linear isomers, and toxicity studies do not consider the influence of the branched isomers. However, since PFAS bioaccumulation is facilitated by protein transporters (Forsthuber et al., 2020), it is likely that binding affinities and toxicity vary among isomers. It is also well known that structural isomers of organic chemicals significantly affect their biological activities. Therefore, the isomeric distribution of PFAS cannot be neglected as it may impact negative health effects, resulting in higher or lower potency compared with their linear counterparts. The findings in this study not only underscore the importance of fundamental scientific research but also create opportunities for engineering applications to carry out bioremediation of persistent halogenated compounds such as PFAS.

4. Conclusion

To date, *L. portucalensis* strain F11 is one of the few isolated microorganisms that has been reported to degrade PFAS successfully, as evidenced in the biodegradation of PFOS, 6:2 FTS, and 5:3 FTCA into shorter-chain compounds and production of fluoride ions in the

culture media. Notably, *L. portucalensis* F11 has the ability to degrade both *per*-fluorinated and poly-fluorinated compounds: up to 96 % of spiked PFOS after a 194-day incubation, and 58 % of spiked 5:3 FTCA and 21 % of spiked 6:2 FTS removed after 100 days incubation. Metabolites of PFOS degradation from 7-carbon to 3-carbon: PFHpS, PFHxS, PFHxA, PFPeA, PFBA, and PFPrA were detected in PFOS-spiked media. In 194-day incubation, three de-fluorinated metabolites were identified: PFOS-F (m/z = 480.940), PFOS-2F (m/z = 462.980), and unsaturated PFOS-3F (m/z = 442.943). During the degradation of 5:3 FTCA, several metabolites were formed: PFHxA, PFPeA, PFBA, PFPrA, 5:3 FTUCA, and 7:2 FTUCA. In 6:2 FTS-spiked media, 4:2 FTS was detected. While further experiments are needed to evaluate the ability of *L. portucalensis* F11 in degrading a wide range of "forever chemicals", results from this study lay the foundation for optimizing analytical conditions to understand the mechanism of PFAS biodegradation by *L. portucalensis* F11, which in turn will provide critical insights that will inform the design of effective bioremediation strategies.

CRediT authorship contribution statement

Mindula K. Wijayahena: Writing – review & editing, Visualization, Validation, Methodology, Investigation, Formal analysis, Data curation, Conceptualization. **Irina S. Moreira:** Writing – review & editing, Methodology, Investigation, Formal analysis, Data curation, Conceptualization. **Paula M.L. Castro:** Writing – review & editing, Supervision, Project administration, Funding acquisition. **Sarah Dowd:** Writing – review & editing, Methodology, Formal analysis. **Melissa I. Marciesky:** Writing – review & editing. **Carla Ng:** Writing – review & editing. **Diana S. Aga:** Writing – review & editing, Visualization, Supervision, Project administration, Funding acquisition, Conceptualization.

Declaration of competing interest

The authors declare that there are no financial conflicts of interest or personal relationships that could have influenced the research presented in this paper.

Acknowledgments

This work was supported by the National Institute of Health, National Institute of Environmental Health Sciences (NIEHS Award #R01ES032717). We would also like to thank the scientific collaboration of CBQF under the FCT project UID/Multi/UIDB/50016/2020. Diana S. Aga also acknowledges financial support from Fulbright Global Scholar Award Program.

Appendix A. Supplementary data

Additional chemical, experimental, and instrumental details, including additional mass spectra, repeated sample data. Supplementary data to this article can be found online at https://doi.org/10.1016/j.scitotenv.2024.178348.

Data availability

Data will be made available on request.

References

Amorim, C.L., Moreira, I.S., Maia, A.S., Tiritan, M.E., Castro, P.M., 2014. Biodegradation of ofloxacin, norfloxacin, and ciprofloxacin as single and mixed substrates by *Labrys portucalensis* F11. Appl. Microbiol. Biotechnol. 98 (7), 3181–3190. https://doi.org/10.1007/s00253-013-5333-8.

Barzen-Hanson, K.A., Roberts, S.C., Choyke, S., Oetjen, K., McAlees, A., Riddell, N., McCrindle, R., Ferguson, P.L., Higgins, C.P., Field, J.A., 2017. Discovery of 40 classes of per- and Polyfluoroalkyl substances in historical aqueous film-forming foams (AFFFs) and AFFF-impacted groundwater. Environ. Sci. Technol. 51 (4), 2047–2057. https://doi.org/10.1021/acs.est.6b05843.

Benskin, J.P., Yeung, L.W.Y., Yamashita, N., Taniyasu, S., Lam, P.K.S., Martin, J.W., 2010. Perfluorinated acid isomer profiling in water and quantitative assessment of manufacturing source. Environ. Sci. Technol. 44 (23), 9049–9054. https://doi.org/10.1021/es102582x.

Bokade, P., Gaur, V.K., Tripathi, V., Bobate, S., Manickam, N., Bajaj, A., 2023. Bacterial remediation of pesticide polluted soils: exploring the feasibility of site restoration. J. Hazard. Mater. 441, 129906. https://doi.org/10.1016/j.jhazmat.2022.129906.

Brunn, H., Arnold, G., Körner, W., Rippen, G., Steinhäuser, K.G., Valentin, I., 2023. PFAS: forever chemicals—persistent, bioaccumulative and mobile. Reviewing the status and the need for their phase out and remediation of contaminated sites. Environmental sciences. Europe 35 (1). https://doi.org/10.1186/s12302-023-00721-8.

Buck, R.C., Franklin, J., Berger, U., Conder, J.M., Cousins, I.T., de Voogt, P., Jensen, A.A., Kannan, K., Mabury, S.A., van Leeuwen, S.P.J., 2011. Perfluoroalkyl and polyfluoroalkyl substances in the environment: terminology, classification, and origins. Integr. Environ. Assess. Manag. 7 (4), 513–541. https://doi.org/10.1002/ieam.258.

Camdzic, D., Welgama, H.K., Crawley, M.R., Avasthi, A., Cook, T.R., Aga, D.S., 2023. Rapid capture of per- and Polyfluoroalkyl substances using a self-assembling zirconium-based metal-organic cage. ACS Appl. Eng. Mater. 2 (1), 87–95. https://doi.org/10.1021/acsaenm.3c00592.

Carvalho, M.F., De Marco, P., Duque, A.F., Pacheco, C.C., Janssen, D.B., Castro, P.M.L., 2008. *Labrys portucalensis* sp. nov., a fluorobenzene-degrading bacterium isolated from an industrially contaminated sediment in northern Portugal. Int. J. Syst. Evol. Microbiol. 58 (3), 692–698. https://doi.org/10.1099/ijs.0.65472-0.

Charbonnet, J.A., McDonough, C.A., Xiao, F., Schwichtenberg, T., Cao, D., Kaserzon, S., Thomas, K.V., Dewapriya, P., Place, B.J., Schymanski, E.L., Field, J.A., Helbling, D. E., Higgins, C.P., 2022. Communicating confidence of per- and Polyfluoroalkyl substance identification via high-resolution mass spectrometry. Environ. Sci. Technol. Lett. 9 (6), 473–481. https://doi.org/10.1021/acs.estlett.2c00206.

Chen, Y., Wang, S., Geng, N., Wu, Z., Xiong, W., Su, H., 2022. Artificially constructing mixed bacteria system for bioaugmentation of nitrogen removal from saline wastewater at low temperature. J. Environ. Manag. 324, 116351. https://doi.org/10.1016/j.jenvman.2022.116351.

Chetverikov, S.P., Sharipov, D.A., Korshunova, T.Y., Loginov, O.N., 2017. Degradation of perfluorooctanyl sulfonate by strain *Pseudomonas plecoglossicida* 2.4-D. Appl. Biochem. Microbiol. 53 (5), 533–538. https://doi.org/10.1134/S0003683817050027.

Cook, A.M., Laue, H., Junker, F., 1998. Microbial desulfonation. FEMS Microbiol. Rev. 22 (5), 399–419. https://doi.org/10.1111/j.1574-6976.1998.tb00378.x.

Cordner, A., Goldenman, G., Birnbaum, L.S., Brown, P., Miller, M.F., Mueller, R., Patton, S., Salvatore, D.H., Trasande, L., 2021. The true cost of PFAS and the benefits of acting now. Environ. Sci. Technol. 55 (14), 9630–9633. https://doi.org/10.1021/acs.est.1c03565.

Dagliya, M., Satyam, N., Sharma, M., Garg, A., 2022. Experimental study on mitigating wind erosion of calcareous desert sand using spray method for microbially induced calcium carbonate precipitation. J. Rock Mech. Geotech. Eng. 14 (5), 1556–1567. https://doi.org/10.1016/j.jrmge.2021.12.008.

DiStefano, R., Feliciano, T., Mimna, R.A., Redding, A.M., Matthis, J., 2022. Thermal destruction of PFAS during full-scale reactivation of PFAS-laden granular activated carbon. Remediat. J. 32 (4), 231–238. https://doi.org/10.1002/rem.21735.

Dodds, J.N., Hopkins, Z.R., Knappe, D.R.U., Baker, E.S., 2020. Rapid characterization of per- and polyfluoroalkyl substances (PFAS) by ion mobility spectrometry–mass spectrometry (IMS-MS). Anal. Chem. 92 (6), 4427–4435. https://doi.org/10.1021/acs.analchem.9b05364.

Dutta, N., Usman, M., Ashraf, M.A., Luo, G., Zhang, S., 2022. A critical review of recent advances in the bio-remediation of chlorinated substances by microbial dechlorinators. Chem. Eng. J. Adv. 12. https://doi.org/10.1016/j.ceja.2022.100359.

Forsthuber, M., Kaiser, A.M., Granitzer, S., Hassl, I., Hengstschläger, M., Stangl, H., Gundacker, C., 2020. Albumin is the major carrier protein for PFOS, PFOA, PFHxS, PFNA and PFDA in human plasma. Environ. Int. 137, 105324. https://doi.org/10.1016/j.envint.2019.105324.

Foster, M., Rainey, M., Watson, C., Dodds, J.N., Kirkwood, K.I., Fernández, F.M., Baker, E.S., 2022. Uncovering PFAS and other xenobiotics in the dark metabolome using ion mobility spectrometry, mass defect analysis, and machine learning. Environ. Sci. Technol. 56 (12), 9133–9143. https://doi.org/10.1021/acs.est.2c00201.

Grandjean, P., 2018. Delayed discovery, dissemination, and decisions on intervention in environmental health: a case study on immunotoxicity of perfluorinated alkylate substances. Environ. Health 17 (1), 62. https://doi.org/10.1186/s12940-018-0405-y.

Grandjean, P., Timmermann, C.A.G., Kruse, M., Nielsen, F., Vinholt, P.J., Boding, L., Heilmann, C., Molbak, K., 2020. Severity of COVID-19 at elevated exposure to perfluorinated alkylates. PLoS One 15 (12), e0244815. https://doi.org/10.1371/journal.pone.0244815.

Guardian, M.G.E., Boongaling, E.G., Bernardo-Boongaling, V.R.R., Gamonchuang, J., Boontongto, T., Burakham, R., Arnnok, P., Aga, D.S., 2020. Prevalence of per- and polyfluoroalkyl substances (PFASs) in drinking and source water from two Asian countries. Chemosphere 256, 127115. https://doi.org/10.1016/j.chemosphere.2020.127115.

Halwatura, L.M., Aga, D.S., 2023. Broad-range extraction of highly polar to non-polar organic contaminants for inclusive target analysis and suspect screening of environmental samples. Sci. Total Environ. 893, 164707. https://doi.org/10.1016/j.scitotenv.2023.164707.

Harding-Marjanovic, K.C., Houtz, E.F., Yi, S., Field, J.A., Sedlak, D.L., Alvarez-Cohen, L., 2015. Aerobic biotransformation of fluorotelomer thioether amido sulfonate

(Lodyne) in AFFF-amended microcosms. Environ. Sci. Technol. 49 (13), 7666–7674. https://doi.org/10.1021/acs.est.5b01219.
Huang, S., Jaffe, P.R., 2019. Defluorination of Perfluorooctanoic acid (PFOA) and Perfluorooctane sulfonate (PFOS) by *Acidimicrobium* sp. strain A6. Environ. Sci. Technol. 53 (19), 11410–11419. https://doi.org/10.1021/acs.est.9b04047.
Izquierdo-Sandoval, D., Fabregat-Safont, D., Lacalle-Bergeron, L., Sancho, J.V., Hernandez, F., Portoles, T., 2022. Benefits of ion mobility separation in GC-APCI-HRMS screening: from the construction of a CCS library to the application to real-world samples. Anal. Chem. 94 (25), 9040–9047. https://doi.org/10.1021/acs.analchem.2c01118.
Kwon, B.G., Lim, H.J., Na, S.H., Choi, B.I., Shin, D.S., Chung, S.Y., 2014. Biodegradation of perfluorooctanesulfonate (PFOS) as an emerging contaminant. Chemosphere 109, 221–225. https://doi.org/10.1016/j.chemosphere.2014.01.072.
Lewis, R.C., Johns, L.E., Meeker, J.D., 2015. Serum biomarkers of exposure to Perfluoroalkyl substances in relation to serum testosterone and measures of thyroid function among adults and adolescents from NHANES 2011–2012. Int. J. Environ. Res. Public Health 6098–6114.
MacNeil, A., Li, X., Amiri, R., Muir, D.C.G., Simpson, A., Simpson, M.J., Dorman, F.L., Jobst, K.J., 2022. Gas chromatography-(cyclic) ion mobility mass spectrometry: a novel platform for the discovery of unknown per-/Polyfluoroalkyl substances. Anal. Chem. 94 (31), 11096–11103. https://doi.org/10.1021/acs.analchem.2c02325.
Mancinelli, M., Martucci, A., Ahrens, L., 2023. Exploring the adsorption of short and long chain per- and polyfluoroalkyl substances (PFAS) to different zeolites using environmental samples. Environ. Sci.: Water Res. Technol. 9 (10), 2595–2604. https://doi.org/10.1039/D3EW00225J.
Mendez, V., Holland, S., Bhardwaj, S., McDonald, J., Khan, S., O'Carroll, D., Pickford, R., Richards, S., O'Farrell, C., Coleman, N., Lee, M., Manefield, M.J., 2022. Aerobic biotransformation of 6:2 fluorotelomer sulfonate by *Dietzia aurantiaca* J3 under sulfur-limiting conditions. Sci. Total Environ. 829, 154587. https://doi.org/10.1016/j.scitotenv.2022.154587.
Moreira, I.S., Amorim, C.L., Carvalho, M.F., Castro, P.M., 2012a. Degradation of difluorobenzenes by the wild strain *Labrys portucalensis*. Biodegradation 23 (5), 653–662. https://doi.org/10.1007/s10532-012-9541-1.
Moreira, I.S., Amorim, C.L., Carvalho, M.F., Castro, P.M.L., 2012b. Co-metabolic degradation of chlorobenzene by the fluorobenzene degrading wild strain Labrys portucalensis. Int. Biodeterior. Biodegradation 72, 76–81. https://doi.org/10.1016/j.ibiod.2012.05.013.
Moreira, I.S., Ribeiro, A.R., Afonso, C.M., Tiritan, M.E., Castro, P.M., 2014. Enantioselective biodegradation of fluoxetine by the bacterial strain *Labrys portucalensis* F11. Chemosphere 111, 103–111. https://doi.org/10.1016/j.chemosphere.2014.03.022.
Mullin, L., Jobst, K., DiLorenzo, R.A., Plumb, R., Reiner, E.J., Yeung, L.W.Y., Jogsten, I. E., 2020. Liquid chromatography-ion mobility-high resolution mass spectrometry for analysis of pollutants in indoor dust: identification and predictive capabilities. Anal. Chim. Acta 1125, 29–40. https://doi.org/10.1016/j.aca.2020.05.052.
Muter, O., 2023. Current trends in bioaugmentation tools for bioremediation: a critical review of advances and knowledge gaps. Microorganisms 11 (3). https://doi.org/10.3390/microorganisms11030710.
Nzila, A., Razzak, S.A., Zhu, J., 2016. Bioaugmentation: an emerging strategy of industrial wastewater treatment for reuse and discharge. Int. J. Environ. Res. Public Health 13 (9). https://doi.org/10.3390/ijerph13090846.
Ober, C.K., Käfer, F., Deng, J., 2022. Review of essential use of fluorochemicals in lithographic patterning and semiconductor processing. J. Micro/Nanopattern. Mater. Metrol. 21 (01). https://doi.org/10.1117/1.Jmm.21.1.010901.
Organtini, K.L., Rosnack, K.J., Hancock, P., 2023. Expanding the Range of PFAS in a Single Injection to Include Ultra Short Chains Using the Atlantis™ BEH™ C_{18} AX Mixed Mode Column. Waters Corporation. https://www.waters.com/content/dam/waters/en/app-notes/2023/720008034/720008034-en.pdf (accessed 01/03/2024).
Özel Duygan, B.D., Gaille, C., Fenner, K., van der Meer, J.R., 2021. Assessing antibiotics biodegradation and effects at sub-inhibitory concentrations by quantitative microbial community deconvolution. Front. Environ. Sci. 9. https://doi.org/10.3389/fenvs.2021.737247.
Presentato, A., Lampis, S., Vantini, A., Manea, F., Dapra, F., Zuccoli, S., Vallini, G., 2020. On the ability of Perfluorohexane sulfonate (PFHxS) bioaccumulation by two *Pseudomonas* sp. strains isolated from PFAS-contaminated environmental matrices. Microorganisms 8 (1). https://doi.org/10.3390/microorganisms8010092.
Prevedouros, K., Cousins, I.T., Buck, R.C., Korzeniowski, S.H., 2006. Sources, fate and transport of perfluorocarboxylates. Environ. Sci. Technol. 40 (1), 32–44. https://doi.org/10.1021/es0512475.
Rios-Bonilla, K.M., Aga, D.S., Lee, J., Konig, M., Qin, W., Cristobal, J.R., Atilla-Gokcumen, G.E., Escher, B.I., 2024. Neurotoxic effects of mixtures of perfluoroalkyl substances (PFAS) at environmental and human blood concentrations. Environ. Sci. Technol. 58 (38), 16774–16784. https://doi.org/10.1021/acs.est.4c06017.
Shaw, D.M.J., Munoz, G., Bottos, E.M., Duy, S.V., Sauve, S., Liu, J., Van Hamme, J.D., 2019. Degradation and defluorination of 6:2 fluorotelomer sulfonamidoalkyl betaine and 6:2 fluorotelomer sulfonate by *Gordonia* sp. strain NB4-1Y under sulfur-limiting conditions. Sci. Total Environ. 647, 690–698. https://doi.org/10.1016/j.scitotenv.2018.08.012.
Taniyasu, S., Kannan, K., Horii, Y., Hanari, N., Yamashita, N., 2003. A survey of perfluorooctane sulfonate and related perfluorinated organic compounds in water, fish, birds, and humans from Japan. Environ. Sci. Technol. 37 (12), 2634–2639. https://doi.org/10.1021/es0303440.
Vieira, V.M., Hoffman, K., Shin, H.M., Weinberg, J.M., Webster, T.F., Fletcher, T., 2013. Perfluorooctanoic acid exposure and cancer outcomes in a contaminated community: a geographic analysis. Environ. Health Perspect. 121 (3), 318–323. https://doi.org/10.1289/ehp.1205829.
Yang, S.H., Shi, Y., Strynar, M., Chu, K.H., 2022. Desulfonation and defluorination of 6:2 fluorotelomer sulfonic acid (6:2 FTSA) by *Rhodococcus jostii* RHA1: carbon and sulfur sources, enzymes, and pathways. J. Hazard. Mater. 423 (Pt A), 127052. https://doi.org/10.1016/j.jhazmat.2021.127052.
Yi, L.B., Chai, L.Y., Xie, Y., Peng, Q.J., Peng, Q.Z., 2016. Isolation, identification, and degradation performance of a PFOA-degrading strain. Genet. Mol. Res. 15 (2). https://doi.org/10.4238/gmr.15028043.
Yu, Y., Zhang, K., Li, Z., Ren, C., Chen, J., Lin, Y.H., Liu, J., Men, Y., 2020. Microbial cleavage of C-F bonds in two C(6) per- and polyfluorinated compounds via reductive defluorination. Environ. Sci. Technol. 54 (22), 14393–14402. https://doi.org/10.1021/acs.est.0c04483.
Yu, Y., Xu, F., Zhao, W., Thoma, C., Che, S., Richman, J.E., Jin, B., Zhu, Y., Xing, Y., Wackett, L., Men, Y., 2024. Electron bifurcation and fluoride efflux systems implicated in defluorination of perfluorinated unsaturated carboxylic acids by *Acetobacterium* spp. Sci. Adv. 10 (29), eado2957. https://doi.org/10.1126/sciadv.ado2957.
Zhang, S., Lu, X., Wang, N., Buck, R.C., 2016. Biotransformation potential of 6:2 fluorotelomer sulfonate (6:2 FTSA) in aerobic and anaerobic sediment. Chemosphere 154, 224–230. https://doi.org/10.1016/j.chemosphere.2016.03.062.

Sustainable PFAS Mitigation Using Hemp and Soil Additives

Paula Carrera[1,2], Erik De Bruyn[1], Farideh Yarahmadi[1], Andrew Jimenez[1], Filip Cordeel[1], Frederik Verstraete[1], Ingmar Nopens[1,2]

[1] C-Biotech, Frank Van Dyckelaan 15, 9140 Temse (Belgium)

[2] BIOMATH, Ghent University, Coupure Links 653, 9000 Ghent (Belgium)

ABSTRACT

PFAS contamination presents significant environmental challenges and requires effective treatments. In the case of polluted soils, phytoremediation using industrial hemp offers a promising alternative, given its rapid growth and capacity for pollutants uptake. This study aimed to optimize PFAS mitigation via hemp by evaluating its ability to extract, degrade or stabilize PFAS, while exploring different targeted soil treatments in open field trials, including fungi and additives for germination, foliage and root growth stimulation. The overall PFAS and PFOS removal efficiency after one cultivation cycle was 67%, bringing most plots below the Flemish remediation standard. Short-chain PFAS were more readily taken up by the above-ground plant parts, and preferentially accumulated in the leaves. On the other hand, long-chain PFAS were removed from the soil but not accumulated in the plant, suggesting effective removal based on degradation into shorter compounds prior to uptake. Based on these observations, a new BioConversion Accumulation Factor (BCAF) was proposed to account for the plant accumulation of degradation products. The applied soil treatments improved phytoremediation by influencing plant physiology and PFAS accessibility. In particular, the use of germination additives led to the presence of shorter chain PFAS and the highest accumulation in the plant tissues, with BAF up to 27.14 total PFAS, and BAF and BCAF for PFOS of 0.83 and 1.8, respectively. Overall, these findings confirm the significant potential of industrial hemp as an effective, scalable, nature-based solution for PFAS phytoremediation, when combined with the right soil additives.

Keywords: PFAS, Hemp, Soil Remediation, Phytoremediation, Nature-Based Solutions, BioConversion Accumulation Factor

1. INTRODUCTION

Per- and polyfluoroalkyl substances (PFAS) are a group of man-made chemicals known for their resistance to heat, water, and oil. They have been used extensively in various industries since the 1940s in a wide range of products, including non-stick cookware, water-repellent clothing, stain-resistant fabrics, and firefighting foams (Wang et al., 2017, Kucharzyk et al., 2017). However, their persistence in the environment and resistance to natural degradation processes have led to widespread contamination of soil and water systems (Wee and Aris, 2023, Nason et al., 2024). For these reasons, they are often called "forever chemicals" (Kucharzyk et al. 2017, Nason et al., 2024). PFAS in the environment presents significant risks to human health and ecosystems. Exposure to these highly stable organic compounds, characterized by strong carbon-fluorine bonds (Schaider et al., 2017), has been associated with numerous adverse health effects, and thus, there is an urgent need to develop effective methods for the remediation of PFAS-contaminated sites (Kucharzyl et al. 2017, Rheay et al. 2021, Nason et al., 2024, Wee and Aris, 2023).

Various methods have been developed for PFAS remediation, including adsorption, filtration, thermal treatment, chemical oxidation/reduction, and soil washing (de Bruecker, 2015; Kucharzyk et al., 2017; Mahinroosta and Senevirathna, 2020). While these approaches have shown promise in laboratory studies, their cost-effectiveness and field feasibility remain uncertain. Moreover, most commercial methods focus on groundwater rather than soil remediation. As these methods are suitable mainly for ex situ treatment, the excavation of the soil top layers is required, and leads to transportation and logistical challenges which have a significant carbon footprint. Moreover, the soil is lost after treatment and needs to be replaced. Thus, these methods often tend to be expensive or impractical for in situ implementation.

This is also the case in Belgium, in which PFAS soil contamination presents significant environmental challenges. After the investigation of this issue began in Belgium, several

property owners and government authorities faced land decontamination demands. Using trucks and heavy machinery for dredging contaminated soil causes noise and pollution, and additional landfill capacity is limited. In addition, due to groundwater contamination, even in the case of soil excavation, pollution can potentially return when groundwater levels increase. Therefore, finding effective and sustainable solutions has become necessary.

In situ bioremediation, which employs biological agents to remove contaminants, offers a potentially simple, environmentally friendly, and cost-effective solution for PFAS-contaminated soils. This method treats contamination in situ, reducing post-cleanup costs significantly (Shahsavari et al., 2019). Bioremediation has been successfully applied to various organic pollutants, such as petroleum hydrocarbons, chlorinated substances, and pesticides (Adetutu et al., 2015; Uqab et al., 2016; Khudur et al., 2019), but its application to PFAS is still limited, highlighting a critical research gap for advancing soil bioremediation technologies.

Phytoremediation has emerged as a promising bioremediation approach for addressing PFAS contamination. This technique relies on plants to absorb, collect, and occasionally break down pollutants in the soil and water (Nason et al., 2024, Gobelius et al., 2017, Shahsavari et al., 2021). Several plant species have been shown to absorb PFAS (Nason et al., 2024; Nassazi et al., 2022; Dusza, 2023, Xu, et al., 2022). For example, Zhang et al. (2019) found that *Betula pendula* and *Picea abies* showed significant PFAS accumulation, while the wetland species *Juncus effusus* accumulated 11.4% of seven PFAS compounds from a soil spiked with PFAS. Although phytoremediation does not lead to substantial degradation of PFAS, bioaccumulation of PFAS in plants is a viable means of removing them from contaminated environments (Huff et al., 2020, Shahsavari et al., 2021).

Industrial hemp (*Cannabis sativa*) has shown potential for PFAS phytoremediation due to its fast growth, high biomass production and ability to accumulate contaminants. It is an invaluable resource for many conventional and contemporary industrial products such as food,

fiber, oil, and medication (Tilkat et al., 2023). This plant is tolerant of temperatures between 13 and 22 °C, and it is highly adaptable to many growing locations and soil types, especially heavy-alkaline soils. However, it prefers soils that are deep, well-aerated, with a pH of 6, and having sufficient moisture and nutrients (Rehman et al., 2021, Dutt et al., 2003).

Recent studies have explored the effectiveness of hemp in PFAS phytoremediation. Nassazzi et al. (2022) observed accumulation in the hemp leaves of 0.0008–7.4 μg/g DM in pot trials and quantified the number of cycles needed to achieve a certain removal efficiency. However, the initial concentrations used were very high (14 mg/kg DM), being at least one or two orders of magnitude higher than mildly or diffuse contaminated sites. Nason et al. (2024) investigated hemp phytoremediation on a former military base and observed PFAS accumulation in the stems. Nevertheless, the tested hemp varieties did not reach maturity, which likely explains these observations and makes the conclusions of the study unreliable, including the claim that phytoremediation is not a viable technology. The importance of understanding the uptake mechanisms and the factors influencing PFAS accumulation in plants (Lesmeister et al., 2021) and investigating the potential of the amendments with plants (Nassazi et al., 2022) have been documented as well. Although hemp has a significant ability to absorb PFAS, previous studies have shown that the types of PFAS that tend to be absorbed by plants are water-soluble and tend to leach through the soil (Dusza, 2023). Therefore, the use of technologies that can convert these contaminants in the soil into a soluble form could increase the availability of the absorbable form and increase absorption rates and removal from the soil. Thus, despite the promising results of hemp ability for PFAS remediation, further research is needed to unravel the uptake and possible degradation mechanisms and find the best conditions for optimal removal.

This study aims to evaluate the effectiveness of industrial hemp in PFAS removal from soil and test soil additives that can optimize the process by enhancing uptake. For this purpose, the

following specific objectives were defined: (1) confirmation of previously reported uptake of PFAS from soil and storage in the leaves as well as quantification of bioaccumulation factors for different PFAS types, (2) evaluation of the removal efficiency of PFAS from soil, and (3) optimization of remediation methods to improve PFAS uptake and accelerate cleanup, making it a scalable and sustainable phytoremediation technique.

2. MATERIALS AND METHODS

2.1. Site Description

The study was conducted at the Vesta Campus, a multidisciplinary training center for safety professionals (e.g. firefighters) in Ranst, Belgium. Due to this long-term land use, the soil at Vesta was detected as significantly contaminated with PFAS, well above the Flemish remediation standard (3.8 µg/kg DM). The initial PFAS concentrations across the study area ranged from 0.5 to 29 µg/kg DM, with an average of 12.3 µg/kg DM. The soil texture consists of a sand-loam mixture covered with a thin layer of transferred soil slightly contaminated with stone rubble. The initial soil properties were 0.65 mg NO_3-N/kg DM, 1.48 mg NH_4-N/kg DM, 84% of dry matter content, 1.09 % of organic carbon and a pH of 5.7 (Tauw, 2024).

2.2. Experimental Design

An open-field experiment was conducted on a site sized approximately 0.3 ha, using the industrial hemp variety Futura 83. The experiment consisted of 9 plots (Figure 1) designed to evaluate the impact of hemp phytoremediation with and without some selected additives and PFAS removal in a natural field setting. Based on our technical studies, different soil treatments were applied, consisting of additives with potentially desired properties enhancing PFAS uptake (Table 1). In particular, 5 biobased additives (Ad) were tested: Ad1 is a biocatalyst which speeds up biochemical processes, Ad2 speeds up germination, Ad3 stimulates foliage, Ad4 stimulates root development and Ad5 is a fungus present at the site, supposed to shorten

PFAS chain length. All plots except plot 3 (a blank of non-treated soil seeded with hemp) were treated before the seeding with a fertilizer specifically formulated by the partner company Bertels B.V. based on a soil nutrient analysis. Details of this cannot be disclosed.

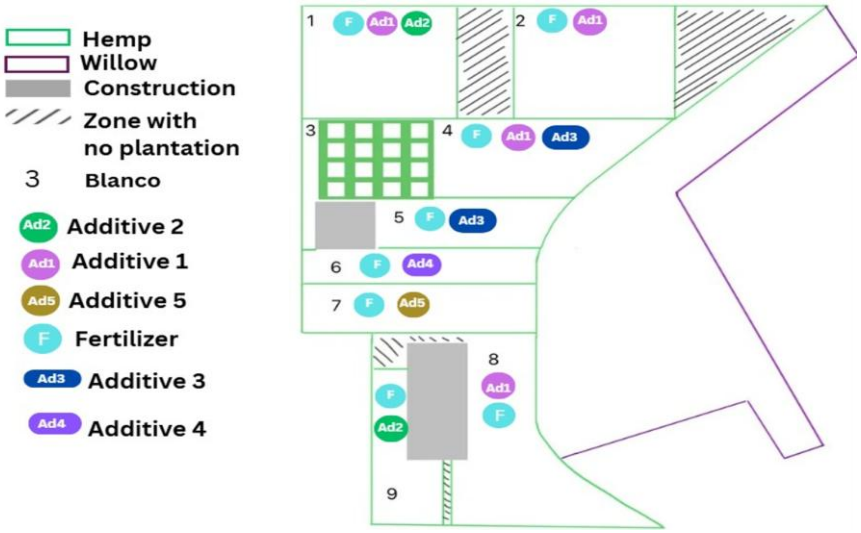

Figure 1: Experimental design at the Vesta site. The purple line at the right indicates willows.

The locations of the different treatments were chosen randomly, but ensuring the presence of a buffer zone among them to minimize the risk of cross contamination of the different additives. The shapes and sizes were selected based on physical obstacles present in the plot. The green squared location was used to set up small replicas of the nine open field plots, without interaction with the groundwater. These small plots were used to support the observations made in the open field plots. To mitigate the risk of PFAS leaching into groundwater and spreading to the surrounding environment, which could occur through the working mechanism of some of the additives, 1,000 willow trees were planted downstream of the hemp field (purple lines to the right of Figure 1). These trees act as a secondary barrier, further reducing environmental risks.

Table 1. Soil Treatments Applied in the Experiment.

Plot	Treatment	Additive dosage
1	Hemp + Ad1+ Ad2 + fertilizer	Ad1: 13 L/1000 m^2, added 3 times, Ad2: 30 kg/1000 m^2
2	Hemp+ Ad1+ fertilizer	Ad1: 13 L/1000 m^2, added 3 times
3	Control, Hemp	-
4	Hemp + Ad1 + Ad3 + fertilizer	Ad1: 13 L/1000 m^2, added 3 times Ad3: 2 L/1000 m^2 after the first leaves
5	Hemp+ Ad3+ fertilizer	2 L/1000 m^2 after the first leaves
6	Hemp+ Ad4 + fertilizer	5 L/1000 m^2
7	Hemp+ Ad5 + fertilizer	No dosage, present onsite
8	Hemp + Ad1 (no fertilizer)	Ad1: 13 L/1000 m^2, added 3 times
9	Hemp + Ad2+ fertilizer	30 kg/1000 m^2

No irrigation was required during the experiment due to the unusually wet Spring and Summer of 2024. However, excessive rainfall in certain lower areas of the field restricted plant growth, highlighting the impact of site-specific conditions.

2.3. Monitoring and Sampling

Soil and Plant Sampling

Soil samples were collected using a soil auger, with all the equipment cleaned using PFAS-free detergent (Deconex 11) between samples to prevent contamination. In all 9 plots, one fixed sampling location was marked (based on GPS coordinates) for consistent and repeatable sampling minimizing the potential impact of pollution heterogeneity, and samples were transported in coolers to preserve integrity. Additionally, 9 mixed samples (1 per plot) were taken of 3 random subsamples per plot, to assess pollution heterogeneity within each plot. Soil samples were collected at two depths: 20 cm and 50 cm. The 20-cm samples were used to monitor PFAS distribution and uptake dynamics over time. The 50-cm samples were used to assess PFAS leaching into the soil. Baseline measurements were taken in May and early June, followed by monthly samples until September (Table 2).

Plant sampling focused on hemp leaves only, since this plant part is known for its ability to accumulate short-chain PFAS (Nassazzi et al., 2023) and based on our previous experience that

indicated that no PFAS occurred in the stems. Diagonal sampling was used within each plot for consistency. A diagonal line across the field was chosen to represent a cross-section of different areas of each plot. Then, all 5 individual samples were mixed to form a composite sample, with approximately 50 g of plant material collected per plot. Samples were stored in coolers during transport to prevent degradation. Samples were collected monthly (June–September) to evaluate PFAS uptake during the growth stages: seedling, vegetative, pre-flowering, and maturation (Table 2).

Table 2: Soil and Leaf Sampling Chronogram.

Date	Soil sampling	Leaves sampling (plant growth stage)
23/5/2024	Baseline measurement	
3/6/2024	Baseline measurement	
3/7/2024		Sampling 1 (seedling)
24/7/2024		Sampling 2 (vegetative)
29/7/2024	Sampling 1	
31/7/2024	Mixed Sampling 1	
7/8/2024	Mixed Sampling 2	
26/8/2024	Sampling 2	
27/8/2024		Sampling 3 (pre-flowering)
12/9/2024	Sampling 3	
12/9/2024	Mixed Sampling 3	Sampling 4 (maturity)

Plant Growth and Harvesting

Plant growth was monitored in 2 ways, being the biomass yield and drone-based Normalized Vegetation Difference Index (NVDI), to evaluate vegetation health and biomass production. Two drone flights were conducted, one at mid-growth season to assess plant development during peak vegetative stages and one just before harvesting to evaluate final biomass production. Meteorological conditions were carefully recorded in a logbook.

To prevent recontamination from falling leaves, hemp plants were harvested at the end of the experiment using mechanical mowers. Biomass was collected and transported for controlled PFAS disposal via pyrolysis. A total of 3 tons of wet biomass was harvested, resulting in approximately 300 kg of dried and pelletized leaves.

2.4. Laboratory Analysis

Soil and plant samples were analyzed at SGS Belgium NV following an in-house multi-step approach to comprehensively analyze PFAS in soil samples. First, EOF (Extractable Organo Fluorine) Screening provided an overall indication of the presence of PFAS in the sample. Next, a target analysis was performed using LC-MS/MS in compliance with the CMA/3/D protocol for precise quantification of PFAS. 42 PFAS compounds were analyzed, 31 of which were measured quantitatively and 11 were determined qualitatively (Table S1). The detection limits where 200 µg/kg for EOF and 0.5 µg/kg DM per compound for the target analysis. In this study, the EOF analysis was only performed at the start of the experiment, as the measured concentrations were below the detection limit.

2.5. Calculations

Bioaccumulation Factors

The bioaccumulation factor (BAF) was calculated as the ratio between the PFAS concentration measured in the leaves at the end of the experiment ($C_{PFAS,L,t=end}$, µg/kg DM) and the PFAS concentration in the soil at the beginning of the experiment ($C_{PFAS,S,t=0}$, µg/kg DM) (Eq.1).

$$BAF = \frac{C_{PFAS,L,t=end}}{C_{PFAS,S,t=0}} \quad \textbf{Eq. 1}$$

To account for the accumulated degradation products of specific PFAS compounds, a bioconversion and accumulation factor (BCAF) is proposed in this study. This way, the sum of the concentrations of the degradation products (i) is added to the compound concentration in the leaves, calculated as follows using PFOS as an example:

$$BCAF_{PFOS} = \frac{C_{PFOS,L,t=end} + \sum C_{i,L,t=end}}{C_{PFOS,S,t=0}} \quad \textbf{Eq. 2}$$

Mass Balance Calculations

The mass balances were set up (both per total PFAS and PFOS) to assess the mass removed from the soil ($m_{PFAS,S,rem}$, µg) due to transport and reaction pathways: accumulation in the plant (A), transformation (R) and leaching (LC) (Figure 2). The general mass balance was formulated according to Eq.3.

$$m_{PFAS,S,rem} = \left(C_{PFAS,S,t=0} - C_{PFAS,S,t=end}\right) \cdot m_S = A + R + LC \qquad \textbf{Eq. 3}$$

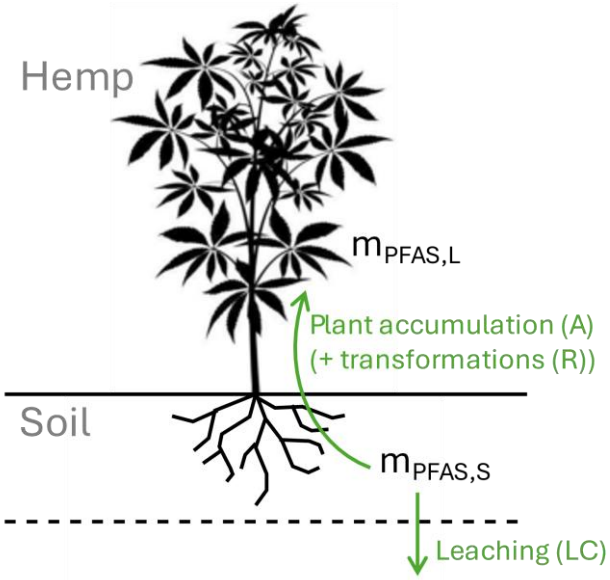

Figure 2. PFAS pathways considered in the mass balance.

Where $C_{PFAS,S,t=0}$ is the initial PFAS concentration in the soil (µg/kg DM) and $C_{PFAS,S,t=end}$ is the final PFAS concentration in the soil (µg/kg DM). The mass of soil (m_S, kg) was calculated by considering the volume of soil, the bulk density and the dry matter content (DMC_S).

$$m_S = V_S \cdot \rho_S \cdot DMC_S \qquad \textbf{Eq. 4}$$

Where V_S is the volume of the soil (m^3), calculated as the product of the parcel area (A_P, m^2) and the depth (h_P, m) and ρ_S is the soil bulk density (kg/m^3).

The accumulated PFAS (A) refer to those present in the leaves, as no PFAS were detected in stems and roots. The mass of PFAS in the leaves ($m_{PFAS,L,t=end}$, µg) was calculated as the product

of the measured concentration at the end of the field trial ($C_{PFAS,L,t=end}$, µg/kg DM) and the mass of harvested leaves (m_L, kg DM):

$$m_{PFAS,L,t=end} = C_{PFAS,L,t=end} \cdot m_L \quad \textbf{Eq. 5}$$

Where m_L was calculated as the product of the total harvested mass (m_H) and the fraction of leaves (f_L), taking into account the dry matter content (DMC_L).

$$m_L = m_H \cdot f_L \cdot DMC_L \quad \textbf{Eq. 6}$$

Leaching (LC) was considered negligible in the mass balance based on soil measurements at different soil depths. The input data used for these calculations is shown in Table 3.

Table 3: Input Data for Mass Balance Calculations.

Parameter	Description	Value	Units	Source
ρ_S	Soil bulk density	1.5	kg/dm^3	Assumed
A_P	Parcel area (per plot)	375	m^2	Measured
h_P	Parcel depth	0.2	m	Assumed
DMC_S	Dry matter content of the soil	84	%	Measured
DMC_L	Dry matter content of the leaves	20	%	Measured
f_L	Fraction of leaves in the harvest	20	%	Assumed
m_H	Total harvested mass per plot	318	kg	Measured

The amount of PFAS accumulated in the leaves was compared to the removed PFAS, by calculating their ratio from the general mass balance (Eq. 3).

$$\text{Accumulated fraction (\%)} = \frac{A}{m_{PFAS,S,rem}} \cdot 100 = \frac{m_{PFAS,L,t=end}}{m_{PFAS,S,rem}} \cdot 100 \quad \textbf{Eq. 7}$$

The accumulated fraction of PFOS was calculated similarly, but also considering the amount of degradation products in the leaves ($m_{i,L,t=end}$, µg).

$$\text{Accumulated fraction (\%)} = \frac{A}{m_{PFOS,S,rem}} \cdot 100 = \frac{m_{PFOS,L,t=end} + \sum m_{i,L,t=end}}{m_{PFOS,S,rem}} \cdot 100 \quad \textbf{Eq. 8}$$

Degradation Yields

The degradation yields of PFOS were calculated from previous studies as the ratio of the mass of the product ($C_{i,t=end}$, µg/L or µg/kg DM) and the initial reactant concentration ($C_{PFOS,t=end}$, µg/L or µg/kg DM) (Eq. 9). The yields were calculated individually per each degradation compound. The same calculation was applied to calculate the yield of produced PFOS from precursors degradation.

$$\text{Degradation yield} = \frac{C_{i,t=end}}{C_{PFOS,t=0}} \qquad \textbf{Eq. 9}$$

3. RESULTS AND DISCUSSION

3.1. PFAS Dynamics and Removal from the Soil

The initial soil PFAS concentrations measured in this study showed significant differences for the different plots, contradicting the initial information available from the study area, stating similar values of PFAS throughout the site. This presents a caveat regarding the experimental design, which assumed a rather homogeneous pollution in the site. The measured PFAS concentrations varied between 0 – 32 µg/kg DM depending on the plot (Figure 3, more details on spatial distribution in Figures S1, S2). PFOS was the dominant compound in almost all of the plots, accounting for 45 – 100 % of the initial PFAS concentrations, except for plot 5, where 6:2 FTS was the main detected PFAS compound. In addition, in plots 7 – 9, a significant fraction of shorter chain compounds was also present in the soil.

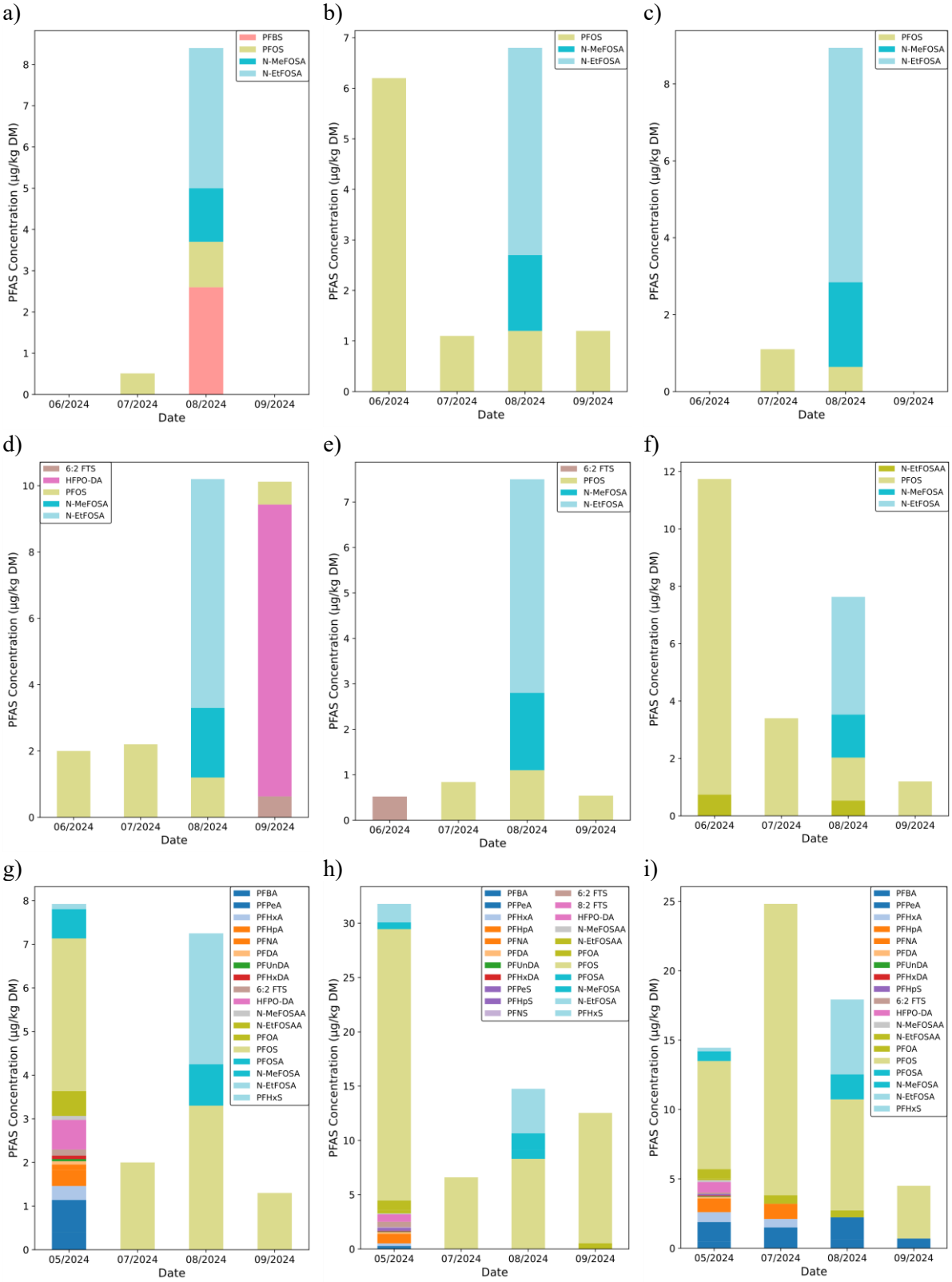

Figure 3. Monthly PFAS Concentration and Composition Dynamics Throughout the Experiment in Plots 1 – 9 (a – i, respectively).

For most plots a decrease in PFAS concentration was observed after one month (Figure 3). However, in August most of the plots exhibited an increase, after which a final decrease occurred in September. A couple of reasons could explain this increase in concentration. First, in mid-July (12/7/2024), the site was hit by a hailstorm, resulting in hemp plants being literally decapitated, causing those parts of the plant biomass to fall onto the soil. Degradation of this biomass could have set free the PFAS that had been taken up and, hence, result in an increase in the amount of PFAS in the soil in some plots. This increase could be due to the cutting of branches and the scattering of a large number of leaves on the soil and their decomposition. This could have caused an increase of the soil organic matter, which is an important sorbent for PFAS (Xu et al., 2022). A second and even more plausible hypothesis is the entry of PFAS from outside the site along with contaminated runoff. In August, a forbidden Sulfluramid pesticide (N-EtFOSA) was applied to a neighboring site (beyond the control of the authors), which explained the increase in the PFAS concentration in the soil. This intrusion was clearly observed in the analyses performed in August due to the sudden appearance of the long-chain compounds N-MeFOSA and N-EtFOSA, with similar concentrations of 5 – 8 μg/kg DM in all plots which were not present anywhere in the site in July (Figure 3).

Despite this, plants were able to grow again after the storm, and the PFAS concentrations measured in September decreased up to 90% after one month. The only exception was plot 4, where the total PFAS concentrations remained almost unchanged due to the intrusion of GenX, which was also beyond the authors' control. This was evident from the elevated fraction of HFPO-DA detected in the sample. Throughout the whole experiment, a clear decrease in the concentration of long-chain PFAS was observed in all plots. In addition, the short chain PFAS were also completely depleted. Overall, an average removal efficiency of 67% was observed at site level with respect to the start of the experiment. All treatments significantly reduced the PFAS concentration, and in 7 out of 9 plots, the concentration reached the legal limit in Flanders

of 3.8 µg/kg DM after one cultivation cycle, which is quite remarkable. The median values of all plots dropped from 5.6 µg/kg DM in June to 1.2 µg/kg DM in September (Figure 4a).

The PFOS concentrations also decreased during the experiment, following similar trends, with an average removal efficiency of 67% (Figure 4b). Across all of the plots, the changes in plots 2, 9, and 6 were such that they could be reduced to the legal standard or even lower.

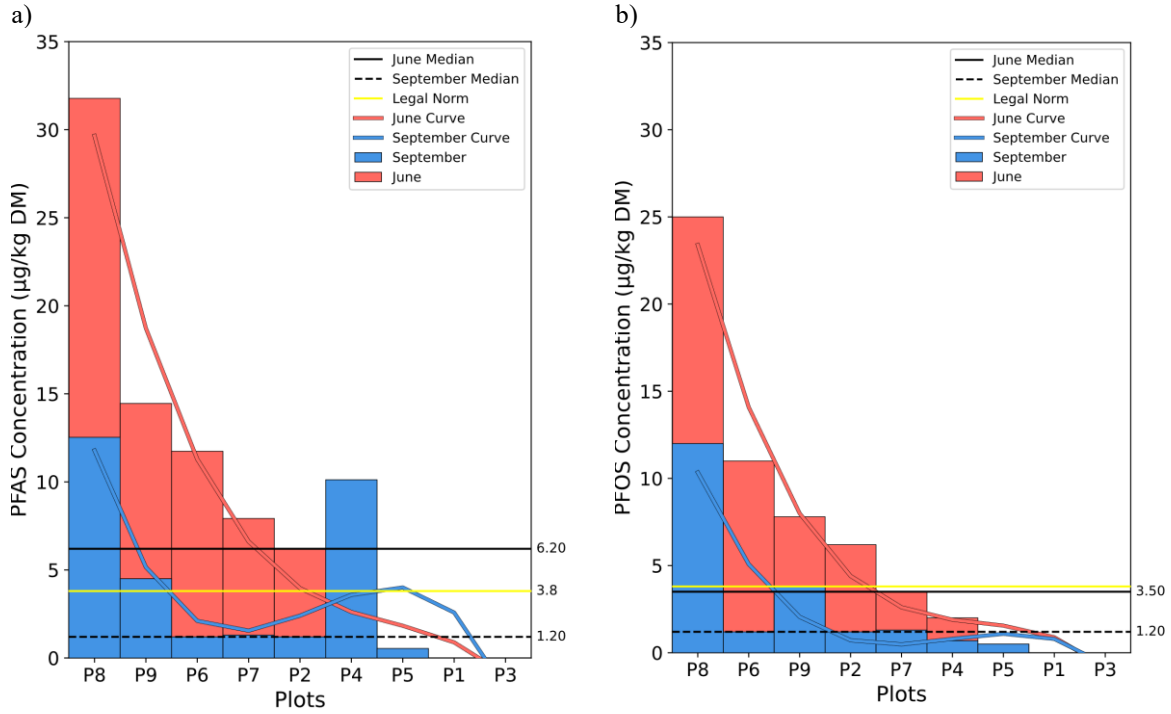

Figure 4. Temporal Changes in the Concentration of a) Total PFAS and b) PFOS at the Beginning and End of the Experiment in Each Plot.

The positive effect of hemp on PFAS-affected lands and its ability for PFAS uptake has been observed in previous studies. Nassazzi et al. (2023) reported PFAS uptake ranging from 0.2 – 33% per crop cycle, and accumulation in hemp, preferentially in the leaves, up to 20 – 40 µg/g DM. Note that their initial concentrations (1.5 mg/kg for each of 10 PFAS compounds) were much higher than average concentrations in soil, usually reported to be below 250 µg/kg (Brusseau et al., 2020; Wellmitz et al., 2023). Consequently, they estimated long time periods (9 - 240 cycles) needed to reach 90% PFAS removal. Nason et al. (2024) also used hemp for PFAS phytoremediation from soil, reaching approximately 1.4 mg of PFAS removed from the

soil via uptake into hemp. However, a maximum of 2% of the initial PFAS was removed from the soil. One important point in this study was the low growth of the hemp plant. Except for one variety that reached 1.2 m in height, the average height of the hemp in the other varieties studied was 30 cm, which seems to indicate that the plant growth in the experiment was not even close to optimal. This very likely negatively impacted PFAS removal, as the biomass and plant growth are effective factors in phytoremediation (Xu et al., 2022). Compared with these studies, much higher removal efficiencies were achieved in this study with only one cultivation cycle, demonstrating the capability of hemp for effective PFAS remediation when combined with the optimal soil additives.

3.2. Soil-Plant Interactions

This study provides important insights into the soil-plant interactions that influence the behavior of PFAS during phytoremediation with industrial hemp. The results indicate a complex interplay of precursor degradation, chain length dynamics and plant uptake and shed light on mechanisms that improve the remediation process. These observations also show that soil treatments can create favorable conditions for the transformation of precursors and subsequent uptake by plants.

PFAS Accumulation in Leaves

PFAS accumulation in the leaves was observed in all plots, with total concentrations in the leaves between 9 – 66 µg/kg DM at the end of the experiment, except in plot 9, where much higher concentrations up to 380 µg/kg DM were detected (Figure 5). The dominant compounds in the leaves were short-chain PFAS, especially PFBA and PFPeA. Longer chain PFAS were observed as well in some plots, but in much lower concentrations, which has been also confirmed by previous studies (Xu et al., 2022) and is related to the higher hydrophobicity of longer-chain molecules. The long-chain PFAS fractions in the leaves were the highest at the beginning, and decreased in some plots throughout the experiment (Figure S.5). This was

probably due to further degradation in the leaves through the oxidation, reduction or hydrolysis of these compounds as part of the metabolic processes of the plant (Xu et al., 2022). PFAS compounds with chain lengths higher than 9 were not detected.

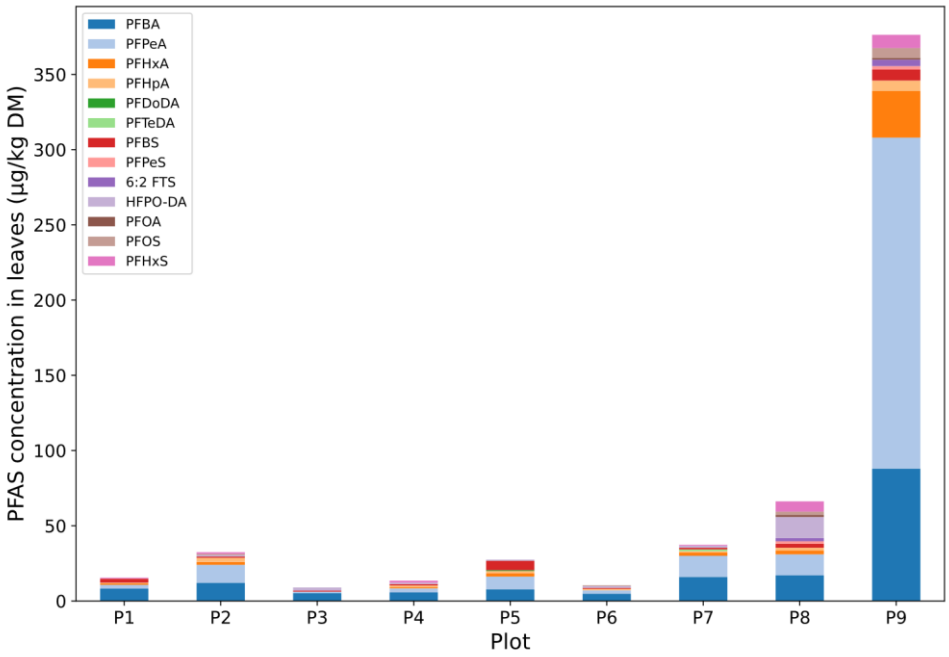

Figure 5. PFAS Accumulation in the Leaves in Each Plot at the End of the Experiment.

The Bioaccumulation Factor (BAF) varied considerably among the specific PFAS compounds and across plots (Table 4). The highest BAFs were observed in plot 9, where hemp could be considered a hyperaccumulator for 5 compounds (6:2 FTS, PFBA, PFHxA, PFHxS and PFPeA) given that a BAF higher than 10 was observed (Huff et al. 2020). In addition, it had the highest BAF for PFOS of 0.83, far exceeding the other plots. This indicates an increased bioavailability and/or a more active transport into the plant due to the applied treatment and the dynamics of precursor conversion. Hemp cultivated in plots 8 and 7 also showed its capability as a hyperaccumulator of 5 (HFPO-DA, PFBA, PFHxA, PFPeA, PFPeS) and 2 (PFBA, PFPeA) compounds, respectively. These results are in line with previous studies using hemp for PFAS remediation, which reported the accumulation of the same or similar compounds. Nassazzi et al. (2023) reported hemp to be a hyperaccumulator for PFBA, PFPeA, PFHxA, PFBS, and PFHxS, among others, and Nason et al. (2024) also observed BAF higher

than 10 for PFBA, PFPeA, and PFHxA. High BAF of PFBA, PFPeA, PFHxA, PFBS and PFPeS were also observed by Wright et al. (2025).

The BAF of PFOS obtained in this study, in particular in plot 9, are in line with previous studies using different plants for PFAS remediation and higher than values for hemp reported in literature of 0.13 (University of Minnesota, 2022). Felizeter et al. (2012) reported PFOS accumulation of 0.50 ± 0.31 µg/kg f.w. in lettuce leaves, while Liu et al. (2019) reported PFOS concentrations in soybean leaves of 2.35 µg/kg. Additionally, Blaine et al. (2013) calculated BAF for PFOS of 1.67 and 0.32 in lettuce. These results are in line with this study, where the PFOS concentrations in the leaves were 0.5 – 6.5 µg/kg DM, and the BAF were up to 0.83.

Table 4: Bioaccumulation Factors (BAF) for PFAS Compounds.

Plot	6:2 FTS	HFPO-DA	PFBA	PFHpA	PFHxA	PFHxS	PFOA	PFOS	PFPeA	PFPeS
1	-	-	-	-	-	-	-	-	-	-
2	-	-	-	-	-	-	-	0.14	-	-
3	-	-	-	-	-	-	-	-	-	-
4	-	-	-	-	-	-	-	0.00	-	-
5	0.00	-	-	-	-	-	-	-	-	-
6	-	-	-	-	-	-	-	0.05	-	-
7	0.00	1.91	40.00	2.78	6.56	4.67	0.00	0.00	18.92	-
8	4.29	25.45	106.25	3.60	10.83	4.00	1.63	0.09	116.67	22.97
9	43	0.00	179.59	9.45	43.66	33.85	1.79	0.83	157.14	-

Note that the BAF without a number correspond to compounds not initially detected in the soil.

In addition to the direct accumulation of individual PFAS, expressed with the BAF, the accumulation in the plant of short-chain compounds not initially present in the soil was also observed. For instance, the soils in plots 1, 7, 8 and 9 initially showed a dominance of PFOS, with negligible concentrations of shorter-chain sulfonic acids such as PFHxS and PFBS. However, post-harvest analysis revealed a significant increase in the plant tissues, indicating a preferential absorption and accumulation in above-ground plant tissues, consistent with their higher mobility and bioavailability. This aligns with the in-situ transformation of PFOS precursors into more mobile and bioavailable compounds prior to uptake, and corroborates with previous studies that have reported these compounds as PFOS degradation products (Wijayahena et al., 2025; Kwon et al., 2014). In contrast, plot 5 showed mainly PFBA, PFPeA,

PFHxA and PFBS in the leaves without detectable PFOS in the soil, suggesting alternative precursor pathways involving 6:2 FTS. Indeed, PFBA, PFPeA and PFHxA have been identified as degradation products of 6:2 FTS under aerobic conditions (Harding-Marjanovic et al. 2015; Méndez et al., 2022).

These observations clearly indicate transformation of longer chain PFAS into smaller chain ones, which, to the best of our knowledge has not been reported before in a phytoremediation study. However, this transformation and additional plant uptake is not reflected in the BAF, as this parameter only refers to individual compounds. Thus, the BAF underestimates the real accumulation in the plant as it does not account for the degradation products. This shows the need for re-thinking and expanding the definition of bioaccumulation factors. For this reason, we introduce the BioConversion and Accumulation Factor (BCAF, Eq. 2) for compounds that undergo degradation. When the degradation products PFBS and PFHxS are incorporated into the calculation, the BCAFs of PFOS increases to 4.6, 6.3, 0.8, 0.3, 0.2 and 1.8 for plots 2, 4, 6, 7, 8, 9, respectively. In addition, accounting for the degradation products in plot 5 resulted in a BCAF of 35.4 for 6:2 FTS, while the BAF was zero and none of the possible degradation products had an associated BAF.

The BAF of total PFAS also varied considerably between plots, reflecting differences in soil treatment and the presence of precursors. Plot 9 had the highest BAF of 27.14, followed by plots 5, 2 and 7 (Table 5). Note that in plots 1 and 3, no BAF were calculated due to the absence of PFAS at the start of the experiment. The same applies to plot 5, where the PFAS concentration was almost zero. Overall, the BAF was dependent on the chain length of the PFAS compounds, being higher for the shorter chain length PFAS (Figure 6). This trend was observed in all the plots where PFAS accumulation was detected, and is in line with previous studies (Felizeter et al., 2014). However, big differences were observed in the absolute values, especially for chain lengths shorter than 6, associated to the different soil treatments.

Table 5. Overall PFAS Removal, Bioaccumulation and Plant Growth of Each Plot.

Plot	PFAS removal (%)	PFOS removal (%)	PFAS BAF	PFOS BAF	NVDI
1	-	-	-	-	0.88
2	81	81	5.16	0.14	0.88
3	-	-	-	-	0.77
4	0	66	6.50	0	0.85
5	0	-	51.92*	0	0.86
6	90	89	0.83	0.05	0.86
7	84	63	4.67	0	0.86
8	59	52	2.06	0.09	0.88
9	68	51	27.14	0.83	0.91

* High value as a result of the low initial PFAS concentration, close to zero (0.52 µg/kg DM)

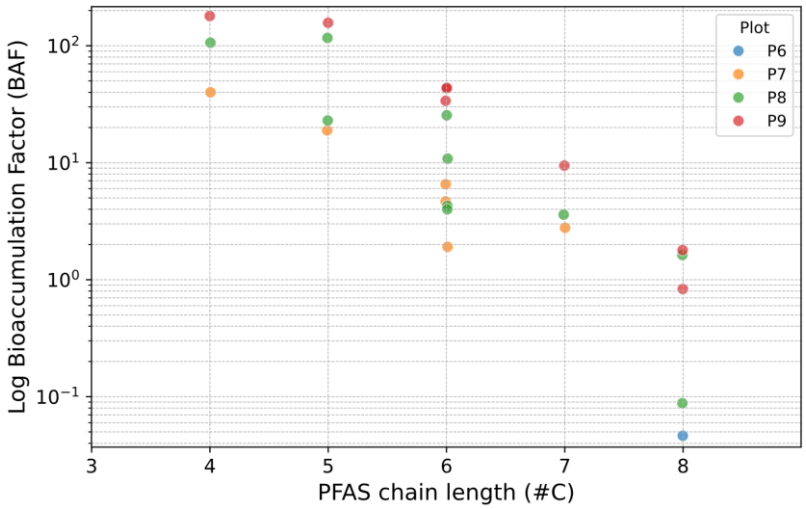

Figure 6. BAF as a Function of the PFAS Chain Length.

To confirm the preferential PFAS accumulation in the leaves, as reported in previous studies (Nassazzi et al., 2023), the PFAS concentration in the roots was measured in plot 6, as it was expected to be the plot with the highest concentrations due to the dosed additive (roots growth enhancement). However, PFOS was the only compound detected, with concentrations in the side roots of 1.9 and 2.3 µg/kg DM of L-PFOS and T-PFOS, respectively, and no PFAS detected in the main roots. Given the significantly low PFAS concentrations in the roots compared to the leaves in plot 6, the rest of plots were expected to have even less relevant concentrations.

The soil-plant interactions observed in this study, suggesting long-chain PFAS degradation and uptake, were probably due to a complex synergic effect of soil properties, plant, and microbial communities in the soil. Bacteria often found in the root zone of plants, can degrade and

detoxify these pollutants and thus contribute to the remediation of contaminated environments (Nason et al., 2024). In addition, the root exudates of plants are associated with the uptake of PFAS by the root. For instance, oxalic acid in root exudates was found to play a key role in activating PFOA uptake in lettuce, which Xiang et al. (2020) demonstrated to be more than 80%. The more oxalic acid was contained in the root exudates, the more PFOA was bioaccumulated in the plant. Wen et al. (2013) found that the nonlinear absorption of PFOS and PFOA closely follows the Michaelis-Menten model, suggesting that PFAS uptake by roots is likely a carrier-mediated process (Yang et al., 2010). Additionally, Wang et al. (2020) concluded that PFAS are likely transported through water and anion channels, as the pore diameter matches the size of the C-F bond. Accordingly, factors such as soil properties, species of PFAS and plants are influencing factors of the transport rate of this process (Xu et al., 2022). In addition, plant height, evapotranspiration potential, and other morphological and physiological differences between different plant species probably influence the accumulation potential of PFAS from the soil, which should be considered in future studies (Xu et al., 2022). Therefore, in our study, it seems that two main processes caused the reduction of PFAS in the soil, one is the defluorination of long-chain into short-chain forms (Wijayahena et al., 2025), likely in the rhizosphere, and the other is the direct plant absorption of the short-chain PFAS and part of the long-chains. Additionally, the likely presence of mycorrhiza might have enhanced both degradation and the transport into the roots (Bonfante and Genre, 2010).

Plant Growth

Considerable plant growth was observed in all plots, with an average plant height up to 3 meters and Normalized Difference Vegetation Index (NDVI) close to 1. In particular, a clear success concerning plant growth was observed in plot 9 (with an additive that speeds up germination), with the highest NDVI. Hemp plants were observed to grow taller on the slope along the eastern border of the field, which extended across multiple plots where different additives were

applied. This observation suggests that physical conditions, such as the terrain, may influence the effectiveness of additives. In this case, the slope likely facilitated better drainage of excess rainfall during the exceptionally wet spring and early summer, creating conditions that may have enhanced plant growth independently of the applied treatments. This highlights the need to consider site-specific physical factors when evaluating the performance of additives, as such variables can interact with and potentially modify their effects.

A positive correlation emerged between biomass density and PFAS uptake, with higher biomass generally leading to improved PFAS absorption. Plants in high-density biomass plots demonstrated higher PFAS removal. This is in line with the results of Nassazzi et al. (2022), who found a significant linear relationship ($R2=0.84$, $P<0.0001$) between willow biomass and observation time, which contributed to a continuous increase in PFAS mass accumulation. The results confirm that biomass affects PFAS uptake and plant growth (He et al. 2023).

3.3. Soil-Plant Mass Balances

PFAS Mass Balances

The mass of PFAS removed from the soil ranged from 450 to 1700 mg (Table 6). In plots 1, 3 and 5, no PFAS were detected or their concentrations were very low, and plot 4 was excluded from the analysis since its PFAS concentrations increased by the end of the experiment due to the intrusion of GenX. The mass of PFAS accumulated in the leaves ranged from 0.4 to 4.8 mg, with the highest levels in Plot 9 with the germination additive. However, this accumulation represented only a small fraction of the PFAS removed from the soil across all plots, being less than 1%. This discrepancy likely results from two main factors related to the samples analysis. First, the targeted analysis used in this study could detect only specific PFAS compounds, meaning transformed molecules outside its scope remained undetected. In addition, the samples were below the detection limits of the EOF analysis, thus the amount of PFAS not identified with the targeted analysis could not be determined. Second, ultra-short chain PFAS were not measured in the leaves, but might have supposed a significant mass in the leaves. In addition to the analyses, other factors related to PFAS transport could also contribute to this difference. Firstly, during the storm, the short-chain PFAS could have been leached into the rainwater, and thus not be detected in soil or leaves. In addition, the ultrashort chain PFAS might have been volatilized given the aerobic conditions of the experiment, as reported by Wijayahena et al. (2025). In addition, volatilization might have also occurred during the leaves sampling process and transport for analysis. This could lead to an underestimation of the accumulated amount.

Gaps in the mass balances were also observed in other studies. Nason et al. (2024) also studied PFAS removal from soil using hemp. They reported that 85% of removed PFAS were accumulated in the leaves. In their case, the mass balance was better closed due to the use of a non-targeted analysis (total oxidizable precursor) in combination with a targeted analysis for PFAS quantification. Zhang et al. (2020) studied PFAS removal with *Typha angustifolia* by spiking soil with known PFAS mixtures. Based on their reported concentrations, the mass of

PFAS accumulated in the plants accounted for 4–50% of the PFAS removed from the soil. While both studies were performed with known PFAS mixtures, in our case, the trials were performed with the polluted soil as it was, which implied a wide variety of compounds. In addition, it was an open field test, with external factors which could have affected the experiment. This could explain the bigger gap observed in this case study.

To assess the soil pollution heterogeneity, mass balances were performed using mixed samples collected at the end of the trial (Table 8). These samples generally showed lower PFAS concentrations than single-point samples, suggesting the latter might have been taken from PFAS hotspots within the plots, and a 'dilution effect' of the single point concentrations took place when mixed with the rest of the collected soil in the mixed samples. However, the impact on mass balance calculations was low, with variations between 5 and 20%, and similar fractions of removed PFAS present in the leaves. This indicates that heterogeneity had no significant impact on the mass balances.

Table 6. Soil – Leaves PFAS Mass Balance. Note that only plots where PFAS removal was observed were considered.

Plot #	Initial soil PFAS (mg)	End soil PFAS (mg)	PFAS removed from soil (mg)	End PFAS in leaves (mg)	Transformed PFAS (mg)
Single-point samples					
2	558	108	450	0.41	449.59
6	1057	108	949	0.13	948.47
7	756	117	639	0.24	638.76
8	2880	1170	1710	0.42	1709.58
9	1260	405	855	4.84	850.16
Mixed samples					
2	558	0	558	0.41	557.59
6	1057	54	1003	0.13	1002.47
7	756	63	693	0.24	692.76
8	2880	0	2880	0.42	2879.78
9	1260	531	729	4.84	724.16

Fate of PFOS

Since PFOS was the main compound in most plots, its fate was further assessed by exploring possible degradation pathways from literature, accounting for both precursors and degradation products (Wen at al., 2018; Mejia Avendaño and Liu, 2015; Wijayahena et al., 2025; Chiriac et al., 2023; Kwon et al., 2014; Chetverikov et al., 2017, 2021; Sharipov et al., 2023; Figure 7). This scenario was considered as the microbial mixture from the soil possibly played a significant role in the degradation. Note that only aerobic conversions were taken into account, as soil aerobic conditions are needed for the proper cultivation of hemp.

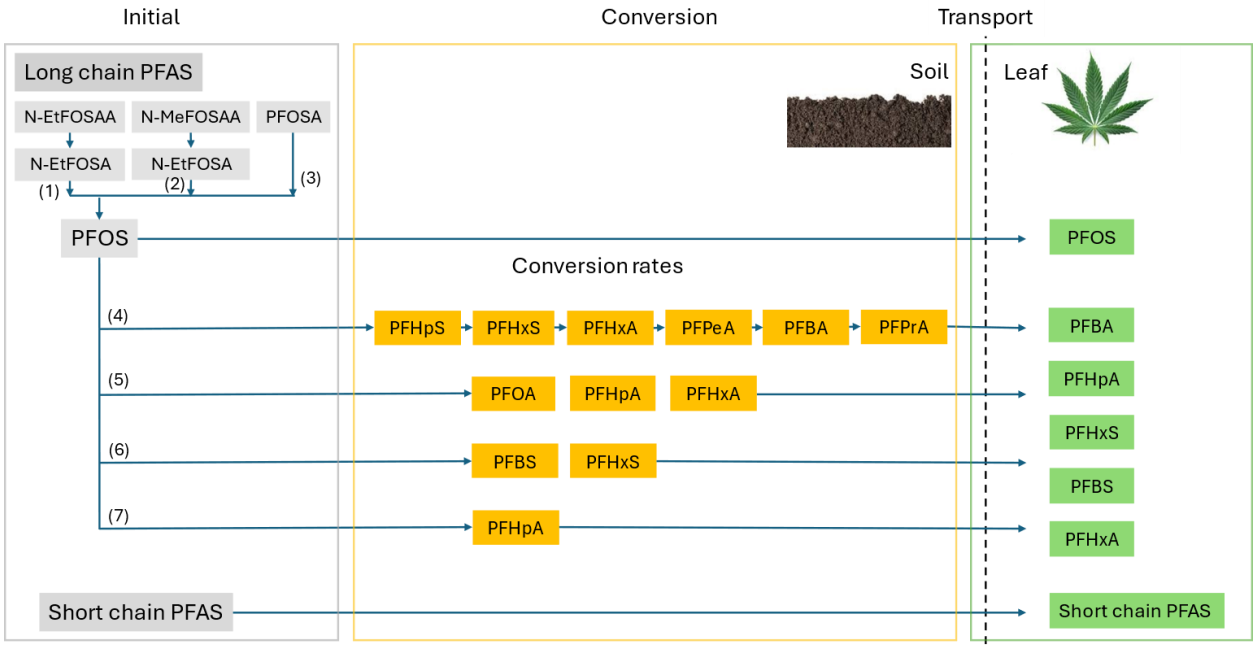

Figure 7. PFOS Production and Degradation Pathways (Numbers indicate each conversion pathway). From (1) Wen at al. (2018), Mejia Avendaño and Liu (2015), (4) Wijayahena et al. (2025), (5) Chiriac et al. (2023), (6) Kwon et al. (2014), (7) Chetverikov et al. (2017, 2021), Sharipov et al. (2023).

The reaction yields, calculated from the information provided in the articles, were found to be quite low in all the pathways, meaning that the degradation products accounted only for a small fraction of the degraded component (Table 7).

Table 7. PFOS Production and Degradation Yields from Literature (Calculated according to Eq. 9).

PFOS precursors						
#	Initial precursor (µg/kg)	Final precursor (µg/kg)	Precursor removal (%)	Produced PFOS (µg/kg)	Yield (g PFOS/g removed precursor)	Reference
1	EtFOSAA: 152	82	46	30	0.43	Wen et al. (2018)
1	EtFOSA: 1650	36	98	61	0.038	Mejia Avendaño and Liu (2015)
PFOS degradation						
#	Initial PFOS (mg/L)	Final PFOS (mg/L)	PFOS removal (%)	Degradation products (µg/L)	Yield (g products/g removed PFOS)	Reference
4	10	0.4	96	PFHpS: 10 PFBA: 70	PFHpS: 0.001 PFBA: 0.007	Wijayahena et al. (2025)
5	1	0.734	26.6	PFHxA: 0 – 0.46	0 – 0.00017	Chiriac et al. (2023)
	0.1	0.053	46.9	PFHxA: 0.26 – 0.38 PFHpA: 0 – 0.21	PFHxA: 0.008 – 0.006 PFHpA: 0 – 0.0045	
6	1400 - 1800	462 - 594	67	PFBS, PFHxS: 0.004 – 0.026*	0.0000037 – 0.000024**	Kwon et al. (2014)
7	1000	0	100	PFHpA: 704***	0.0007	Sharipov et al. (2023), Chetverikov et al. (2021, 2017)

* Specific concentrations per compound not provided. Assumed to be the same for each compound.

** Calculations performed with average initial and final PFOS concentrations

*** Calculated from the reported concentrations of produced fluoride, with a stoichiometry F-:PFHpA 4:1, according to the reaction provided in the articles.

# Indicates the specific pathway from Figure 7.

The mass of PFOS generated from the degradation of the measured precursors (N-MEFOSAA, N-MeFOSA, N-EtFOSAA, N-EtFOSA, PFOSA) was calculated assuming complete conversion to PFOS and 1:1 stoichiometry, given the lack of information on the reaction yields for all the considered pathways. This mass accounted for a small fraction of the PFOS initially present in the soil (Table 8) due to the low precursors' concentrations with respect to PFOS. Consequently, incorporating precursor degradation into the mass balance calculations had a

minimal impact. Note that, when using reported yields, the produced PFOS would be even smaller, and thus have an even smaller impact on the mass balances.

Table 8. Soil – Leaves PFOS Mass Balance. Note that only plots where PFOS removal was observed were considered.

Plot #	Initial soil PFOS (mg)	End soil PFOS (mg)	PFOS removed from soil (mg)	PFOS from precursors (mg)	End leaves PFOS (mg)	Transformed PFOS (mg)*	Attributed to possible degradation pathways (%)
2	558	108	450	0	0.001	449.999	14
6	990	108	882	57	0.006	938.994	7
7	702	117	585	75	0.083	659.917	10
8	2250	1080	1170	87	0.028	1256.972	8.5
9	702	342	360	83	0.083	442.917	24

*Calculated according to Eq.8, 9.

Regarding the PFOS degradation pathways, the available measurements did not allow us to confirm whether degradation occurred, given that the degradation products were also present in the soil. Consequently, the accumulation observed in the leaves could have resulted from both PFOS degradation and uptake from the soil. In addition, almost all the degradation products were present in the leaves at low concentrations, suggesting further transformations. PFBS was the only compound that accumulated in the leaves but was not initially detected in the soil – a degradation product previously reported by Kwon et al. (2014). Considering this pathway, PFBS formation could account for 7–24% of the transformed PFOS in this study, assuming the same yield as that reported by Kwon et al. (2014).

The impact of the different pathways could only be assessed in plot 2, where the PFAS degradation products were initially absent in the soil. In this case, the pathway from Kwon et al. (2014) could account for 7.5%, while that of Wijayahena et al. (2025) would contribute 4.7%, and 1.8% could be attributed to the pathway from Chiriac et al. (2023). As noted above, the amount of PFOS degraded via each pathway may be underestimated due to further transformations of the monitored products into components that were not measured (e.g. ultra short chain PFAS).

The gap between removed PFOS and detected transformation products was also reported in previous studies investigating PFOS degradation with different bacterial strains. These studies consistently reported high PFOS removal efficiencies, yet defluorination products were not always detected. Moreover, all the reported degradation products were present at residual concentrations (3 orders of magnitude lower than the PFOS concentrations). Additionally, unknown degradation products were frequently observed, but their identification and quantification were difficult due to the lack of analytical standards (Wijayahena et al. 2025). This aligns with our findings, which show a clear decrease of the PFOS levels and the presence of degradation products not initially present in the soil, while the total mass of detected degradation products remains significantly lower than the removed PFOS mass.

3.4. Effect of Soil Additives on PFAS Removal and Plant Growth

The different additives used in this study had a clear impact on both plant growth and PFAS removal and uptake. Firstly, they affected the removal rates. After one month, PFAS removal from soil was already observed in 4 of the 7 total treatments (Figure 3), in which the additives had a more direct impact on soil activity, such as roots treatment, fungus and biocatalyst. In contrast, plots treated with additives more focused on plant development (germination, foliage treatments) exhibited slower initial uptake. After the intrusion of the pesticide containing C10 PFAS, in most plots the pesticide-related PFAS were completely removed after one month. The PFAS concentrations decreased considerably in all plots except plot 8, to which the biocatalyst was added. This could indicate that while the biocatalyst may be a useful additive at the start of the experiment, other treatments appear to be more effective once the plant grows. Note that even the blank (plot 3) could remove PFAS after the intrusion, supporting the ability of hemp for soil remediation. In addition, PFAS with chains longer than 10 were removed in all plots, being the main remaining PFAS those with C8 (PFOS). Shorter chain PFAS were removed from the soil as well. Only in plot 9 were shorter PFAS observed in the soil throughout the experiment, which could indicate a better long-chain degradation soil activity.

Plot 6 was the plot with the lowest BAF, despite the high removal efficiency of 90% (Table 6). This is due to the fact that the applied additive focused on improving root growth, which could have meant a better removal from the soil due to root exudates, but not necessarily a better plant uptake. On the other hand, plot 9, to which the germination treatment was applied, showed lower removal efficiencies, but the highest accumulation in leaves and a higher degradation into short chain PFAS. The germination additives (plot 9) empowered hemp to remove PFOS from the soil in an indirect way, through a partial breakdown of PFOS into sulfonic acids with shorter chain lengths, which are more easily absorbed by the plant tissue. At the same time, they also promoted plant growth, reflected in higher NVDI.

All soil treatments helped improve hemp growth, as the blank plot resulted in lower NDVI compared to the rest. Also, P9, with the germination additive, resulted in the highest NDVI, followed by those treatments with biocatalyst (P1, 2, 8).

Based on these results, choosing the right combination of additives is a crucial factor. Among the combinations used, we ultimately know that plot numbers 5, 8 and 9 combinations had a significant effect on increasing the effectiveness of hemp in absorbing long-chain and short-chain pollutants. In addition, it seems that they were able to better withstand the effects of the storm. This seems to indicate that the impact of these treatments was not only on increasing biomass but also led to making PFAS more absorbable or that they increased the root absorption capacity in the rhizosphere environment through the effect on oxalic acid.

3.5. Implications for PFAS Remediation

This study has proven the capability of industrial hemp for PFAS remediation when combined with the optimal soil additives, and documented that the process can be accelerated. Compared to previous studies, PFAS removal was faster, reaching high removal efficiencies after one month, and being able to comply with legal requirements after one cultivation cycle. In particular, germination additives seemed to be the most effective ones to maximize plant

growth, degradation and uptake. These results were likely achieved due to a synergic effect of the hemp, together with the microbial communities and the additives present in the soil. However, further research is needed to confirm these hypotheses, such as soil microbial analysis, which could be linked to degradation pathways. Further unraveling the specific PFAS degradation and uptake mechanisms is also crucial to ensure a faster soil remediation.

The degradation of longer chains into shorter chain PFAS was observed in this study. While shorter-chain PFAS are less bioaccumulative, their increased mobility presents both opportunities and challenges for phytoremediation, and requires a proper characterization of the involved transport processes. On the one hand, their higher plant uptake rates can accelerate remediation efforts. Furthermore, increased dispersion of shorter-chain PFAS in soil and groundwater requires careful management to prevent secondary contamination.

The success of a phytoremediation project, in addition to selecting plants that have sufficient ability to absorb pollutants, also depends on providing appropriate soil additives to make the technique viable (both helping plant growth and changing the form of contaminants into something readily absorbable by the plant). It is also recommended to employ plant species that generate valuable products such as timber, that are either outside the human food chain or manufacture products that are consumed in insufficient quantities to pose a human health risk (Evangelou and Robinson, 2022). Hemp has the potential to be implemented as a comprehensive circular economy solution for land restoration with phytoremediation and using plant residues to manufacture sustainable, recyclable, biobased construction materials. In addition, due to hemp's high ability to capture carbon (Adesina et al., 2020) from atmospheric carbon dioxide, these residues are sequestered in building materials, resulting in a complete, integrated and sustainable management. This is only a viable option when the biomass is free of PFAS. If this cannot be guaranteed, an alternative is to use pyrolysis to destroy the PFAS and create sustainable by-products.

4. CONCLUSIONS

This study highlights the significant potential of industrial hemp as an effective tool for PFAS phytoremediation, especially in combination with targeted soil treatments. Impressive PFAS remediation was achieved, with average removal efficiencies of 67% in a single cultivation cycle, and final concentrations below the legal Flemish standard in most plots.

Similar PFOS removal was achieved, which likely took place through degradation into shorter chain compounds prior to plant uptake. Short-chain PFAS were more readily taken up by the above-ground plant parts compared to long-chain PFAS, which were more likely to remain in the soil due to differences in mobility and bioavailability. Nevertheless, their concentration decreased, meaning they can be removed, albeit in a slower way.

A new BioConversion and Accumulation Factor (BCAF) was proposed in this study, to account for the accumulation of individual compounds and their degradation products.

Soil treatments, especially bio-additives, improved phytoremediation by influencing plant physiology and PFAS accessibility. In particular, the use of germination additives led to the presence of shorter chain PFAS and the highest accumulation in the plant tissues.

5. ACKNOWLEDGMENTS

We would like to express our deepest gratitude to all partners and collaborators who have contributed to this study's success. Our sincere thanks go to Camp Vesta for granting us access to their firefighting training grounds, allowing us to grow industrial hemp, and conduct phytoremediation trials on this PFAS-contaminated site. Our special thanks goes to SGS Belgium for their invaluable support in developing and refining our sampling procedures and for generously providing a comprehensive analysis of the samples collected. Further thanks goes to Bertels B.V. for advising soil preparation and co-developing soil additives to enhance

PFAS uptake. We are also very grateful to Deme Environmental for their continuous support and advice throughout the project. Their expertise played a crucial role in the success of our efforts. Finally, we would like to express our sincere gratitude to Cordeel, under whose umbrella C-Biotech operates, for providing us with the resources and infrastructure necessary to carry out this innovative project. This work is a testament to the power of collaboration, and we are grateful for the trust, knowledge, and commitment of everyone involved.

6. REFERENCES

Adesina, I., Bhowmik, A., Sharma, H., Shahbazi, A. (2020). A Review on the Current State of Knowledge of Growing Conditions, Agronomic Soil Health Practices and Utilities of Hemp in the United States. Agriculture (Basel), 10(4), 129. doi: 10.3390/agriculture10040129

Adetutu, E. M., Gundry, T. D., Patil, S. S., Golneshin, A., Adigun, J., Bhaskarla, V., et al. (2015). Exploiting the intrinsic microbial degradative potential for fieldbased in situ dechlorination of trichloroethene contaminated groundwater. J. Hazard. Mater. 300, 48–57. doi: 10.1016/j.jhazmat.2015.06.055

Blaine, A. C., Rich, C. D., Hundal, L. S., Lau, C., Mills, M. A., Harris, K. M., Higgins, C. P. (2013). Uptake of Perfluoroalkyl Acids into Edible Crops via Land Applied Biosolids: Field and Greenhouse Studies. Environ. Sci. Technol. 47(24), 14062-14069. doi: 10.1021/es403094q

Bonfante, P., Genre, A. (2010). Mechanisms underlying benefi cial plant – fungus interactions in mycorrhizal symbiosis. Nat. Commun. 1:48. doi: 10.1038/ncomms1046

Brusseau, M. L., Anderson, R. H., Guo, B. (2020). PFAS concentrations in soils: Background levels versus contaminated sites. Sci. Total Environ. 740, 140017. doi: 10.1016/j.scitotenv.2020.140017

Chetverikov, S., Sharipov, D. A., Korshunova, T. Y., Loginov, O. N. (2017). Degradation of Perfluorooctanyl Sulfonate by Strain Pseudomonas plecoglossicida 2.4-D. Appl. Biochem. Microbiol. 53(5), 533-538. doi: 10.1134/S0003683817050027

Chetverikov, S., Hkudaigulov, G. (2021). New Ensifer Moralensis h16 strain for perfluorooctane sulphonate destruction. Fluoride 54(4), 309-320.

Chiriac, F. L., Stoica, C., Iftode, C., Pirvu, F., Petre, V. A., Paun, I., Pascu, L. F., Vasile, G. G., Nita-Lazar, M. (2023). Bacterial Biodegradation of Perfluorooctanoic Acid (PFOA) and Perfluorosulfonic Acid (PFOS) Using Pure Pseudomonas Strains. Sustainability 15, 14000. doi: 10.3390/su151814000

de Bruecker, T. (2015). Status report PFOS remediation. DEC Environ. Solutions 12.

Dusza, N. B. (2023). Assessing the potential for hemp to be used in the bioremediation of soils containing perfluoroalkyl substances (PFAS). Master's thesis, University of Arizona, Tucson, USA.

Dutt, D., Singh, V., Ray, A. K., Mukherjee, S. (2003). Development of specialty papers in an Art: Electrical insulation paper from indigenous raw materials – Part IX. J. Sci. Ind. Res., 62: 1145–1151.

Evangelou, M.W. and Robinson, B.H. (2022). The phytomanagement of PFAS-contaminated land. Int. J. Environ. Res. Public Health, 19(11), 6817. doi: 10.3390/ijerph19116817

Felizeter, S., McLachlan, M.S., de Voogt, P. (2012). Uptake of Perfluorinated Alkyl Acids by Hydroponically Grown Lettuce (Lactuca sativa). Environ. Sci. Technol., 46, 11735–11743. doi: 10.1021/es302398u

Felizeter, S., McLachlan, M.S., de Voogt, P. (2014). Root Uptake and Translocation of Perfluorinated Alkyl Acids by Three Hydroponically Grown Crops. J. Agric. Food Chem. 62(115), 3334-3342. doi: 10.1021/jf500674j

Gobelius, L., Lewis, J. and Ahrens, L. (2017). Plant uptake of per-and polyfluoroalkyl substances at a contaminated fire training facility to evaluate the phytoremediation potential of various plant species. Environ. Sci. Technol, 51(21), 12602-12610. doi: 10.1021/acs.est.7b02926

He, Q., Yan, Z., Qian, S., Xiong, T., Grieger, K.D., Wang, X., Liu, C. & Zhi, Y. (2023). Phytoextraction of per- and polyfluoroalkyl substances (PFAS) by weeds: Effect of PFAS physicochemical properties and plant physiological traits. J. Hazard. Mater., 454, 131492. doi: 10.1016/j.jhazmat.2023.131492

Harding-Marjanovic, K. C., Houtz, E. F., Yi, S., Field, J. A., Sedlak, D. L., Alvarez-Cohen, L. (2015). Aerobic Biotransformation of Fluorotelomer Thioether Amido Sulfonate (Lodyne) in AFFF-Amended Microcosms. Environ. Sci. Technol. 49(13), 7666-7674. doi: 10.1021/acs.est.5b01219

Huff, D. K., Morris, L. A., Sutter, L., Costanza, J., and Pennell, K. D. (2020). Accumulation of six PFAS compounds by woody and herbaceous plants: potential for phytoextraction. Int. J. Phytoremediation 22, 1538–1550. doi: 10.1080/15226514.2020.1786004

Khudur, L. S., Shahsavari, E., Webster, G. T., Nugegoda, D., and Ball, A. S. (2019). The impact of lead co-contamination on ecotoxicity and the bacterial community during the bioremediation of total petroleum hydrocarboncontaminated soils. Environ. Pollut. 253, 939–948. doi: 10.1016/j.envpol.2019.0 7.107

Kucharzyk, K. H., Darlington, R., Benotti, M., Deeb, R., and Hawley, E. (2017). Novel treatment technologies for PFAS compounds: a critical review. J. Environ. Manage. 204, 757–764. doi: 10.1016/j.jenvman.2017.08.016

Kwon, B. G., Lim, H., Na, S., Choi, B., Shin, D., Chung, S. (2014). Biodegradation of perfluorooctanesulfonate (PFOS) as an emerging contaminant. Chemosphere 109, 221-225. doi: 10.1016/j.chemosphere.2014.01.072

Lesmeister, L., Lange, F.T., Breuer, J., Biegel-Engler, A., Giese, E., Scheurer, M. (2021). Extending the knowledge about PFAS bioaccumulation factors for agricultural plants– a review. Sci. Total Environ. 766, 142640. doi: 10.1016/j.scitotenv.2020.142640

Liu, Z., Lu, Y., Song, X., Jones, K., Sweetman, A.J., Johnson, A.C., Zhang, M., Lu, X. and Su, C. (2019). Multiple crop bioaccumulation and human exposure of perfluoroalkyl substances around a mega fluorochemical industrial park, China: Implication for planting optimization and food safety. Environ. Int., 127, 671-684. doi: 10.1016/j.envint.2019.04.008

Mahinroosta, R., and Senevirathna, L. (2020). A review of the emerging treatment technologies for PFAS contaminated soils. J. Environ. Manage. 255:109896. doi: 10.1016/j.jenvman.2019.109896

Méndez, V., Holland, S., Bhardwaj, S., McDonald, J., Khan, S., O'Carroll, D., Pickford, R., Richards, S., O'Farrell, C., Coleman, N., Lee, M., Manefield, M. J. (2022). Aerobic biotransformation of 6:2 fluorotelomer sulfonate by Dietzia aurantiaca J3 under sulfur-limiting conditions. Sci. Tot. Environ. 829, 154587. doi: 10.1016/j.scitotenv.2022.154587

Mejia Avendaño, S., Liu, J. (2015). Production of PFOS from aerobic soil biotransformation of two perfluoroalkyl sulfonamide derivatives. Chemosphere, 119, 1084-1090. doi: 10.1016/j.chemosphere.2014.09.059

Nason, S.L., Thomas, S., Stanley, C., Silliboy, R., Blumenthal, M., Zhang, W., Liang, Y., Jones, J.P., Zuverza-Mena, N., White, J.C. and Haynes, C.L. (2024). A comprehensive trial on PFAS remediation: hemp phytoextraction and PFAS degradation in harvested plants. Env. sci., Adv., 3(2), 304-313. doi: 10.1039/D3VA00340J

Nassazzi, W., Lai, F.Y. and Ahrens, L. (2022). A novel method for extraction, clean-up and analysis of per-and polyfluoroalkyl substances (PFAS) in different plant matrices using LC-MS/MS. J Chromatogr B. Analyt. Technol. Biomed. Life Sci., 1212, 123514. doi: 10.1016/j.jchromb.2022.123514

Nassazzi, W., Wu, T.C., Jass, J., Lai, F.Y. and Ahrens, L. (2023). Phytoextraction of per-and polyfluoroalkyl substances (PFAS) and the influence of supplements on the performance of short–rotation crops. Environ. Pollut., 333, 122038. doi: 10.1016/j.envpol.2023.122038

Rehman, M., Fahad, S., Du, G., et al. (2021). Evaluation of hemp (Cannabis sativa L.) as an industrial crop: A review. Environ. Sci. Pollut. Res. Int., 28: 52832-52843. doi: 10.1007/s11356-021-16264-5

Rheay, H.T., Omondi, E.C. and Brewer, C.E. (2021). Potential of hemp (Cannabis sativa L.) for paired phytoremediation and bioenergy production. GCB Bioenergy, 13(4), 525-536. doi: 10.1111/gcbb.12782

Schaider, L. A., Balan, S. A., Blum, A., Andrews, D. Q., Strynar, M. J., Dickinson, M. E., et al. (2017). Fluorinated compounds in U.S. fast food packaging. Environ. Sci. Technol. Lett. 4, 105–111. doi: 10.1021/acs.estlett.6b00435

Shahsavari, E., Rouch, D., Khudur, L.S., Thomas, D., Aburto-Medina, A. and Ball, A.S. (2021). Challenges and current status of the biological treatment of PFAS-contaminated soils. Front. Bioeng. Biotechnol., 8, 602040. doi: 10.3389/fbioe.2020.602040

Shahsavari, E., Schwarz, A., Aburto-Medina, A., and Ball, A. S. (2019). Biological degradation of polycyclic aromatic compounds (PAHs) in soil: a current perspective. Curr. Pollut. Rep. 5, 84–92. doi: 10.1007/s40726-019-00113-8

Sharipov, D., Starikov, S., Chetverikov, S. (2023). Biodefluorination of Perfluorooctanesulphonate by Ensifer adhaerens M1. HAYATI J. Biosci. 30(2) 313-320. doi: 10.4308/hjb.30.2.313-320

Tauw (2024). Onderzoeksverslag PFAS Campus Vesta Ranst.

Tilkat, E., Hoşer, A., Tilkat, E.A., Süzerer, V. and Çiftçi, Y.Ö. (2023). Production of Industrial Hemp: Breeding Strategies, Limitations, Economic Expectations, and Potential Applications. Türk Bilimsel Derlemeler Dergisi, 16(1), 54-74.

University of Minnesota (2022). Understanding and enhancing PFAS phytoremediation mechanisms using hemp plants. Progress in Research presentation. https://clu-

in.org/training/webinar/srppir18/slides/3Slide_Presentation_for_Christy_Haynes,_Ph.D.,_Riley_Lewis,_and_Sara_Nason,_Ph.D.pdf

Uqab, B.,Mudasir, S., and Nazir, R. (2016). Review on bioremediation of pesticides. J Bioremed. Biodeg. 7:343. doi: 10.4172/2155-6199.1000343

Wang, T.T., Ying, G.G., He, L.Y., Liu, Y.S., and Zhao, J.L. (2020). Uptake mechanism, subcellular distribution, and uptake process of perfluorooctanoic acid and perfluorooctane sulfonic acid by wetland plant Alisma orientale. Sci. Total Environ. 733, 139383. doi: 10.1016/j.scitotenv.2020.139383

Wang, Z., DeWitt, J.C., Higgins, C.P. and Cousins, I.T. (2017). A never-ending story of per-and polyfluoroalkyl substances (PFASs)? Environ. Sci. Technol. 51(5) 2508-2518. doi: 10.1021/acs.est.6b04806

Wee, S.Y. and Aris, A.Z. (2023). Environmental impacts, exposure pathways, and health effects of PFOA and PFOS. Ecotoxicol. Environ. Saf., 267, 115663. doi: 10.1016/j.ecoenv.2023.115663

Wellmitz, J., Bandow, N., Koschorreck, J. (2023). Long-term trend data for PFAS in soils from German ecosystems, including TOP assay. Sci. Tot. Environ. 893, 164586. doi: 10.1016/j.scitotenv.2023.164586

Wen, B., Li, L., Liu, Y., Zhang, H., Hu, X., Shan, X.Q., and Zhang, S. (2013). Mechanistic studies of perfluorooctane sulfonate, perfluorooctanoic acid uptake by maize (Zea mays L. cv. TY2). Plant Soil 370, 345–354. http://www.jstor.org/stable/42952672.

Wen, B., Pan, Y., Shi, X., Zhang, H., Hu, X., Huang, H., Lv, J., Zhang, S. (2018). Behavior of N-ethyl perfluorooctane sulfonamido acetic acid (N-EtFOSAA) in biosolids amended soil-plant microcosms of seven plant species: Accumulation and degradation. Sci. Tot. Environ. 642, 366-373. doi: 10.1016/j.scitotenv.2018.06.073

Wijayahena, M. K., Moreira, I. S., Castro. P. M. L., Dowd, S., Marciesky, M. I., Ng, C., Aga, D. S. (2025). PFAS biodegradation by Labrys portucalensis F11: Evidence of chain shortening and

identification of metabolites of PFOS, 6:2 FTS, and 5:3 FTCA. Sci. Tot. Environ. 959, 178348. doi: 10.1016/j.scitotenv.2024.178348

Wright, T., Crompton, M., Bishop, D., Currel, G., Suwal, L., Turner, B. D. (2025). Phytoremediation evaluation of forever chemicals using hemp (Cannabis sativa L.): Pollen bioaccumulation and the risk to bees. Chemosphere, 370, 143859. doi: 10.1016/j.chemosphere.2024.143859

Xiang, L., Chen, X., Yu, P., Li, X., Zhao, H., Feng, N., Li, Y., Li, H., Cai, Q., Mo, C., and Li, Q. (2020). Oxalic acid in root exudates enhances accumulation of perfluorooctanoic acid in lettuce. Environ. Sci. Technol. 54, 13046–13055. doi: 10.1021/acs.est.0c04124

Xu, B., Qiu, W., Du, J., Wan, Z., Zhou, J.L., Chen, H., Liu, R., Magnuson, J.T. and Zheng, C. (2022). Translocation, bioaccumulation, and distribution of perfluoroalkyl and polyfluoroalkyl substances (PFASs) in plants. Iscience, 25(4). doi: 10.1016/j.isci.2022.104061

Yang, C.H., Glover, K.P., and Han, X. (2010). Characterization of cellular uptake of perfluorooctanoate via organic anion transporting polypeptide 1A2, organic anion transporter 4, and urate transporter 1 for their potential roles in mediating human renal reabsorption of perfluorocarboxylates. Toxicol. Sci. 117, 294–302. doi: 10.1093/toxsci/kfq219

Zhang, D., Zhang, W., Liang, Y. (2019). Distribution of Eight Perfluoroalkyl Acids in Plant-Soil-Water Systems and Their Effect on the Soil Microbial Community. Sci. Total Environ., 697, 134146. doi: 10.1016/j.scitotenv.2019.134146

Zhang, D. Q., Wang, M., He, Q., Niu, X., Liang, Y. (2020). Distribution of perfluoroalkyl substances (PFASs) in aquatic plant-based systems: From soil adsorption and plant uptake to effects on microbial community. Environ. Pollut. 257, 113575. doi: 10.1016/j.envpol.2019.113575